Aalto University
School of Chemical
Technology

School of Chemical Technology

Degree Programme of Environomical Pathways for Sustainable Energy Systems (SELECT)

Ricardo Garza Treviño

CATALYTIC UPGRADING OF LIGNIN

Master's thesis for the degree of Master of Science in Technology submitted for inspection, Espoo, 3 August, 2015.

Supervisor **Professor Juha Lehtonen**

Instructor **D.Sc. Reetta Karinen**
Lic. Sc. Johanna Hakonen

Author Ricardo Garza Treviño

Title of thesis Catalyitc upgrading of lignin

Department School of Chemical Technology

Professorship Industrial chemistry **Code of professorship** KE-40

Thesis supervisor Professor Juha Lehtonen

Thesis advisor(s) / Thesis examiner(s) D.Sc. Reetta Karinen
Lic.Sc. Johanna Hakonen

Date 03.08.2015 **Number of pages** 59+08 **Language** English

Abstract

In the broadest vision to contribute to sustainability, with focus on the use of lignin as a sustainable source for the production of chemicals, experiments were performed to find which chemicals may potentially be produced from isolated (organosolv-extracted) lignin through its decomposition by hydrodeoxygenation, as well as to describe the properties and composition of the product as a whole. Catalyst screening was implemented to evaluate the optimal catalyst to obtain low molecular weight organic compounds.

The catalyst screening results of the light bio-oil reaction product fraction showed lowest molecular weights for the experiment involving the Pd/C 3% catalyst with values of 363.4 g/mol of number average and 583.9 g/mol of weight average, as well as fraction of light (monomers and dimers) compounds of 24.1%. The experiment involving the Pd/Al_2O_3 5% showed the highest molecular weights and lowest light compounds fraction.

Regarding the gas product, the experiment involving the Pd/Al_2O_3 5% catalyst exhibited a considerably high amount of methane, and a considerably low amount of hydrogen concentration compared to the other experiments.

In regards to the mass balance of the product streams excluding the gas phase, the Pd/Al_2O_3 5% catalyst showed the highest amount of light bio-oil, however, also the highest amount of char. On the other hand, the lowest amounts of both light bio-oil and char belonged to the experiment involving the Pd/C 3% catalyst.

GC-MS analysis was performed to identify 24 small molecular weight compounds. The most representative compounds for the experiments involving the Pd/C 3%, ZrO_2, and Pd/Al_2O_3 5% catalysts were 4-propylsyiringol, *trans*-4-propenylsyringol, and dihydrosinapyl alcohol, respectively.

Keywords Organosolv lignin, catalytic upgrading, monoaromatics, hydrodeoxygenation

Acknowledgements

My sincere gratitude goes firstly to Professor Juha Lehtonen, for giving me the opportunity to develop this work, and for taking time to give me essential feedback. I also want to thank D.Sc. Reetta Karinen and Research Engineer Heidi Meriö-Talvio for their help and support, as well as valuable feedback. I want to thank as well Syed Farhan Hashmi for providing the lignin used in this experimental work, as well as for his appreciated insights regarding this work.

Very special thanks to Lic.Sc. Johanna Hakonen who designed the experimental methodology, for her uninterrupted help, feedback, comments, and endless support throughout my stay in the Industrial Chemistry research group.

This project was possible with the financial support of Tekes and an Erasmus Mundus scholarship.

Special thanks to my family for having faith in my endeavors.

Espoo, August 3, 2015
Ricardo Garza Treviño

Contents

List of Abbreviations and Symbols

AFEX	Ammonia fiber explosion
APR	Aqueous phase reforming
ARP	Ammonia recycled percolation
BPE	Benzyl phenyl ether
GC-TCD/FID	Gas chromatography with thermal conductivity and flame ionization detection
GC-MS	Gas chromatography – mass spectrometry
HPLC	High performance liquid chromatography
FCC	Fluid catalytic cracking
GPC	Gas permeation chromatography
HDO	Hydrodeoxygenation
HTU	Hydrothermal upgrading
HPLC	High performance liquid chromatography
NMR	Nuclear magnetic resonance
PDI	Polydispersity index
THF	Tetrahydrofuran
VWD	Variable wavelength detector

1. Introduction

Sustainability may be defined as the state in which human activities and way of life can be maintained without exhaustion of resources. Of such resources facing depletion, fossil fuels are of great importance, because not only do they correspond to 80% of the world's primary energy supply[1] [1], but are also utilized to manufacture chemical precursors to a wide variety of products. In this context, biomass is a promising alternative not only as an energy source, but also for the production of bio-based chemicals and materials.

Wood is a lignocellulosic biomass feedstock abundant in nature and considered renewable. It is potentially sustainable when considering optimal periods of growth and harvest, as well as the energy required in all phases of its life cycle.

The main components of lignocellulosic biomass are cellulose, hemicellulose, and lignin, existing both in wood and non-woody biomass such as plant stalks. In general, these constituents range in 40–50% cellulose, 25–30% hemicellulose, and 15–20% lignin [2]. They represent a source of polymers that may be broken into valuable monomeric chemical precursors.

According to the Finnish Forest Research Institute (Metla) [3], 47.4% of consumption of roundwood in 2014 is attributed to the chemical pulp industry. Chemical pulping involves the removal of lignin from wood, which becomes an energy-recoverable waste. The focus of this work is in the use of lignin as a sustainable source for the production of chemicals.

For this purpose, a literature review was carried out in the scope of lignin, its extraction, and decomposition. Experiments were performed to find which chemicals may potentially be produced from isolated (organosolv-extracted) lignin through its decomposition by hydrodeoxygenation, as well as to describe the properties of the product as a whole, including its unidentified components. Cata-

[1] Combined share of oil, coal, natural gas, peat and oil shale in 2012.

lyst screening was implemented to evaluate the optimal catalyst to obtain low molecular weight organic compounds.

LITERATURE REVIEW

2. Lignin

2.1 Structural characteristics

Lignin is a component of the tracheid cell walls of plants – which act as water pipes and mechanical support – that gives strength and water resistance; Lignin also functions as the binding agent of the various cellulose and hemicellulose polysaccharides [4]. A hypothetical depiction of the organization of linkings is shown in Figure 1.

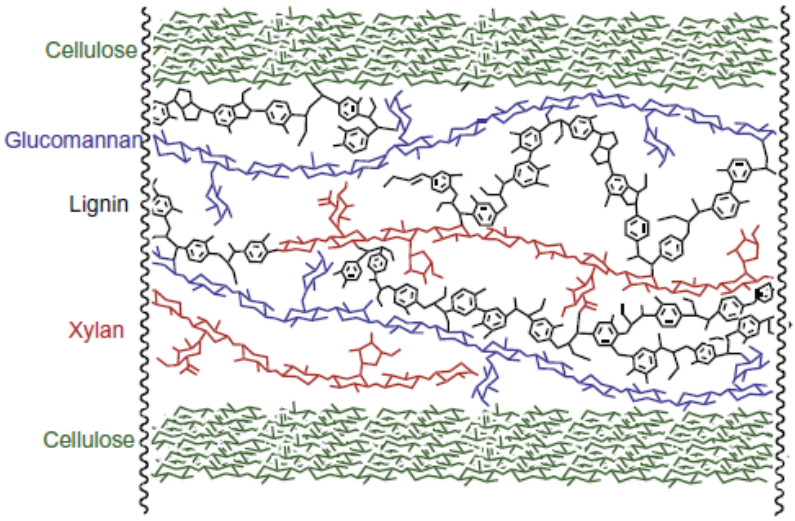

Figure 1. Hypothetical representation of lignin-polysaccharide networks in wood. Reprinted from [4] with permission from Elsevier.

Lignin is a heteropolymer based on phenyl propanoid units of which the main representative monomers are shown in Figure 2. The first from the left, 4-(3-hydroxy-1-propen-1-yl)-2,6-dimethoxy-phenol is also called sinapyl alcohol or syringyl unit. The second, 4-(3-hydroxy-1-propen-1-yl)-2-methoxy-phenol is also called coniferyl alcohol or guaiacyl unit. The third, 4-(3-hydroxy-1-propen-1-yl)-phenol is also called p-coumaryl alcohol or p-hydroxyphenyl unit [4, 5].

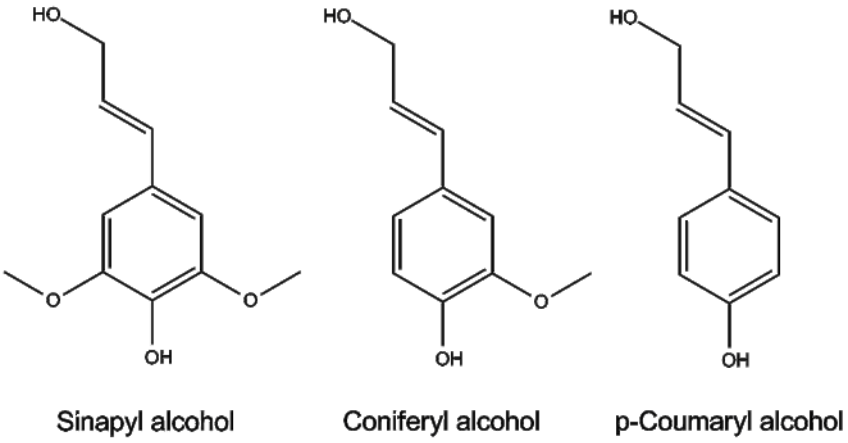

Figure 2. Representative monomeric units of lignin.

The structure of lignin and proportion of its representative monomers is not defined but varies even between taxa and species of the same plant [5]. Herbaceous lignins contain mainly p-hydroxyphenyl units, while lignins from gymnosperm species (softwood) contain mostly guaiacyl units. Angiosperm (hardwood) lignins possess both syringyl and guaiacyl units [6–9].

2.2 Nature of linkages

For the purpose of classifying linkages and substructures, a lignin nomenclature system exists consisting of numbers and Greek letters. As illustrated in Figure 3, the carbons in the aromatic ring are numbered starting from the side chain as number 1. The carbons in the side chain are named with Greek letters starting with the first carbon as α.

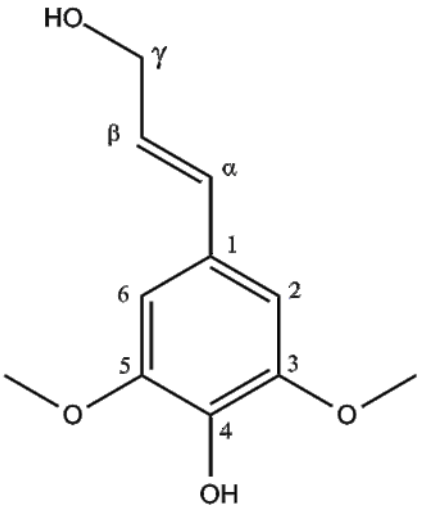

Figure 3. Nomenclature of lignin linkages and substructures.

As mentioned above, the structure of lignin varies depending on its origin and is not completely known. However, analysis by Nuclear Magnetic Resonance (NMR) spectroscopy yields results that may be interpreted to assign quantitative proportions of lignin linkages and substructures.

Table 1. Typical frequency of interlignin linkages. Adapted from [10–12].

Common name/variant	Linkage type	Softwood (%)	Hardwood (%)
β-arylether	β-O-4’	35–60	50–70
α-arylether	α-O-4’	6–8	6–8
Diarylether	4-O-5’	3.5–7	6.5–9
Phenylcoumaran	β-5’	9–12	3–11
Biphenyl	5-5’	9.5–27	3–9
Diarylpropane	β-1’	1–9	1–7
Spirodienone	β-1’	1–3	2–5
Resinol	β-β’	2–6	3–12
Divanillyltetrahydrofuran	β-β’	<1	0

In Table 1, typical proportions of the main linkage types found in softwood and hardwood lignin are presented, accompanied by the common name of the suggested molecules they are part of. Both in softwood and harwood lignin, ether bonds (i.e. β-O-4’, α-O-4’, 4-O-5’) possess the major share, β-O-4’ being the

most common. The other main linkages are C-C bonds, represented by β-5', 5-5', β-1', and β-β'. Of these bonds, β-O-4' is the least resistant to chemical or biological cleavage, while β-5', 5-5', and 4-O-5' are relatively more resistant [13, 11]. Linkage proportions of specific species as well as pretreated wood and lignin (i.e. enzymatic hydrolysis, steam explosion, milling) are reviewed by Laskar and Yang [13], and Du *et al*. [14].

2.3 Extraction

Widely aimed to improve carbohydrates digestability for biofuels production, lignocellulosic biomass fractionation processes may be categorized as physical, physicochemical, biological and chemical. This section is focused in the chemical category.

As mentioned before, around half of the roundwood in Finland is utilized for chemical pulping, which involves the removal of lignin traditionally by inorganic solvents. Less industrially mature procedures to separate lignin include extraction by organic solvents.

2.3.1 Extraction by inorganic solvents

Used as the main chemical techniques to produce pulp for the paper industry, the kraft and sulphite methods rely on inorganic solvents to degrade and dissolve lignin and hemicellulose from wood. Responsible for less than 10% of pulp production in the U.S., the sulphite method dissolves lignin through a combination of sulphurous acid (H_2SO_3) and a salt of sodium (Na), potassium (K), ammonium (NH_4), calcium (Ca) or magnesium (Mg). The by-products of interest are salts of sulphonated lignin called lignosulphonates. [15].

The dominant kraft (or sulphate) process employs sodium hydroxide (NaOH) and sodium sulphide (Na_2S) for the digestion and is suitable for any species of wood. The lignin-containing waste black liquor is combusted to recover energy and afterwards the inorganic pulping chemicals. Increasing the ratio of Na_2S improves delignification by cleavage of β-aryl-ether linkages and methoxy groups but may also increase reduced sulphur emissions and subsequent corrosion of

the recovery system. If the pH of black liquor is “much below 12” lignin may precipitate. [15].

Zhu and Theliander [7] found out that decreasing pH with 6M sulphuric acid (H_2SO_4), increasing ionic strength with sodium sulphate (Na_2SO_4) and/or lower temperatures led to higher precipitated lignin from softwood black liquor in yields up to 86.7%. The lignin precipitation from black liquor (e.g. LignoBoost™) process may be considered to be in the commercial stage [16].

Aside from the two industrial processes mentioned above, laboratory-scale procedures include acid, alkaline, and oxidative treatments. Alkaline hydrolysis by NH_4 and NaOH were reported to remove lignin by 30% and 65% respectively. Other alkalike treatments utilize NaOH and calcium hydroxide ($Ca(OH)_2$), as well as alkaline solution of hydrogen peroxide (H_2O_2), reported to remove 81–88% of lignin after steam explosion pretreatment. [8].

Ammonia recycled percolation (ARP) is a selective process resulting in 40–85% lignin removal in various feedstocks. In the oxidative category ozonolysis has been reported to remove 10–40% lignin while wet oxidation 40–70%. [17].

In laboratory-scale, the most common method for the extraction and determination of lignin content is the Klason acid hydrolysis method [18]. The Klason Lignin method consists of hydrolyzing an extractive-free wood sample with concentrated H_2SO_4. The result is a precipitate of acid-insoluble lignin to be determined gravimetrically, and liquor containing hollocellulose and acid-soluble lignin to measure by UV-Vis spectrometry [19]. A review of experimental conditions from different authors is presented by Sluiter *et al*. [20].

2.3.2 Extraction by organic solvents

The organic category comprises of processes that utilize organic solvents to dissolve lignin, commonly denominated organosolv. These solvents include oxalic, salicylic and acetylsalicylic acid; alcohols, ethers, esters, ketones, glycols, and phenols. Of these, methanol and ethanol are favoured because of their lower boiling point (ease of recovery) and lower cost [8, 17]. Organic acids may cause equipment corrosion and cellulose acetylation [8].

The organic solvent may be combined with an acid or an alkali as catalyst. The extraction by organic solvents is usually carried out at 150–210 ºC. Other process variables include solvent concentration and reaction time [17, 21]. Experiments reviewed by Bundhoo, *et al*. [17] show lignin recovery ranging in 60–80% at varying conditions with ethanol, glycerol, and acetone as base organic solvents. Lignin resulting from organosolv extraction has advantages in its characteristics compared to other extraction processes, listed by Cybulska *et al*. [9] as being highly phenolic, low in carbohydrates, free of sulphur, low in ash, low in molecular weight, and highly hydrophobic.

A unique category of solvents used to fractionate lignocellulosic biomass is ionic liquids. Ionic liquids are organic salts with melting point below 100 ^{0}C formed by organic cations and either organic or inorganic anions. Listed advantages are their physicochemical properties: null flammability, null volatility, high thermal stability, high electrical conductivity [21], high solvating ability; ease of recovery and the possibility to tailor properties such as viscosity, melting point, polarity, and hydrogen bond basicity by changing the combination of cation and anion [22].

Ionic liquids – mostly imidazole-based – have been tested as a pretreatment for biomass to enhance carbohydrates digestability and conversion to biofuels mainly via two ways: 1. Dissolution of complete biomass followed by selective precipitation of cellulose and hemicellulose with water, and 2. Selective extraction of lignin while reducing cellulose crystalinity [22]. Long *et al*. [23] achieved 100% delignification of sugarcane bagasse by ethanol/water (80:20 v:v) in combination with the acidic ionic liquid $[C_4H_8SO_3mimH]HSO_4$.

2.3.3 Other treatments

Physical treatments (i.e. milling, irradiation) are outside the scope of this review because they may have very low or null lignin removal rates [8, 17]. Physicochemical treatments have been presented as pretreatments to improve carbohydrates digestability for biofuels production. Steam explosion at certain conditions has been reported to solubilize 80% of lignin in olive tree wood [17][8] but 11–12% in wheat straw [8]. Ammonia fiber explosion (AFEX) is reported to be inef-

fective especially for biomass with high lignin content [17] and supercritical CO_2 explosion results only report fermentation yields that may or may not be due to delignification [8, 17]. Liquid hot water treatment has been reported to solubilize 40–50% of lignin [24].

Biological methods based on enzymatic hydrolysis are also excluded because they are focused on releasing sugars, and may be considered as postreatment after partial lignin removal by inorganic or organic solvents. Finally, thermochemical methods represent a source of lignin such as tar from pyrolysis.

3. Decomposition and analysis

Most of the extraction methods mentioned above are based on partially breaking the lignin polymer resulting in various smaller molecules. For this reason, the decomposition methods and results will vary considerably depending on their feedstock. Common isolated lignin fractions include dilute acid, alkaline oxidation, pyrolysis, organosolv, sulphite (lignosulphonate), kraft, and physicochemically pretreated (enzymatic hydrolysis residue) lignin. [13, 25].

Decomposition of isolated lignin opens possibilities to produce valuable chemicals from its depolymerization products. Different lignin depolymerization pathways comprise biological and thermochemical processes, in which the latter include purely thermal – gasification, pyrolysis – and catalytic methods: hydrolysis, reduction, oxidation, and cracking. [26, 27].

The catalytic thermochemical methods are reviewed in this section, while biological are outside of the scope. The reason is that although biological decomposition of lignin occurs in nature, challenges need to be overcome before its use in industrial applications. Namely, the restriction to a relatively small range of operating temperatures, instability towards temperature, difficulty to recycle, and high production costs [27, 28]. Regarding purely thermal processes, gasification is outside the scope because the focus of this work is on aromatic monomers, and not gaseous products.

3.1 Hydrolysis

Hydrolysis is a thermochemical treatment that utilizes water for the cleavage of ether bonds in lignin, resulting in phenolic monomers and dimers. This process may be done in presence of a catalyst – acid or alkaline [26] – and at temperatures of 230–370 ^{0}C. Process variables include reaction time, temperature, type of catalyst, and concentration of catalyst. Studies of lignin model compunds show that higher temperatures are required to achieve faster and complete conversion, but may lead to oligomerization (recondensation/recombination of monomers into higher molecular weight oligomers) [27, 29, 31]. Increased residence time also

leads to oligomerization [29, 31]. Catalysts lessen such temperature requirements [30].

Regarding the type of catalyst, Roberts *et al*. [29] found out that addition of alkali carbonates of Li, Na, and K in the hydrolysis of benzyl phenyl ether (BPE) resulted in a decrease in yield of primary phenol and benzyl alcohol and an increase of secondary reaction products toluene and 2- and 4-benzyl phenol compared to the no catalyst case. Toledano *et al*. [32] screened six alkaline catalysts in hydrolysis of olive tree prunings lignin and concluded that all catalysts decreased conversion (increased residual lignin) but also decreased (unwanted) coke formation and increased (desired) oil yield, the latter being highest with NaOH. Roberts *et al*. [31] found out that oil and monomers formation increased with the catalyst – NaOH – concentration and that yield may be further increased by addition of boric acid (H_3BO_3), which prevents oligomerization by forming esters with phenols.

Yang *et al*. [30] compared water-tolerant lewis acids in hydrolysis of model compounds guaiacol, BPE, and diphenyl ether (DPE), and concluded that indium triflate $In(OTf)_3$ resulted in the best conversion and yields of catechol, phenol and benzyl alcohol. Zhu and Zhu [33] screened several catalysts of pure metal powder, metal oxides, metal complexes, phosphines, polyoxometalates, and organic compounds in the hydrolysis of pine wood at 250 ^{0}C and concluded that sodium anthraquinone-2-sulphonate gave the best results: no solid residue or gasification, only small organic acids and aromatics with molecular weight of 162–340.

At pilot scale, hydrothermal treatment at high pressures is used to liquefy biomass into heavy oil to be upgraded into transportation fuel, such as in the Shell Hydrothermal Upgrading (HTU®) process [34].

3.2 Reduction

Reduction techniques are especially suitable for the purpose of utilizing lignin for fuel applications, because they decrease the O/C ratio (0.3–0.4 for lignin, compared to 0.0 for diesel fuel) and increase the H/C ratio (0.7–1.1 respectively for lignin, compared to 2.0 for diesel fuel) while depolymerizing and reducing the carbon chain lengths of the lignin polymer, which in its native form is approxi-

mately $C_{800-900}$ [13]. At industrial scale, hydrogenation or hydroprocessing is used to upgrade lignin based bio-oils from fast pyrolysis or hydrothermal treatment to improve their thermal stability and volatility, as well as to reduce their viscosity [34].

3.2.1 Reaction mechanisms

The hydrodeoxygenation (HDO) process may be considered in two stages: hydrogenolysis (also called direct deoxygenation) and hydrogenation. Catalytic HDO involves treating the sample with hydrogen at high pressures and moderate to high temperatures (200–500 ^{0}C) to break the lignin structure and remove alcohol, aldehyde, ether, and acid functional groups. The hydrogenolysis step produces smaller molecules while maintaining aromaticity and minimizing char formation. This step may be followed then by hydrogenation, which further converts the products into saturated aromatics and aliphatic compounds. The process doesn't necessarily occur in that order, since hydrogenation of the aromatic ring may happen on parallel or before cleaving of the ether bonds. [12, 13, 26].

3.2.2 Catalysts and selectivity

Catalysts used in HDO are mostly heterogeneous, but homogeneous catalysts have also been studied. Studied systems are based mostly in Co-Mo and Ni-Mo catalysts, as well as noble metals [12, 13, 26]. Use of catalysts with high hydrogenation activity, such as precious metal catalysts [13], as well as higher loadings, higher pressures, and higher temperatures result in selectivity to complete hydrogenation instead of hydrogenolysis [27]. Utilizing a catalyst with high selectivity to phenols – such as $NiMo/Al_2O_3$, $RuMo/Al_2O_3$ [12, 13] – would contribute to minimize hydrogen consumption. Another challenge that catalysis may overcome is tolerance to water formation, which may limit their activity [12].

Since the objective is to subject the feedstock to reducing conditions, hydrogen donors are often applied. Formic acid and methanol have been used in the reduction of lignin as well as of lignin model compounds for in situ hydrogen generation. This process is called solvolysis [26]. As catalyst support, alumina (Al_2O_3) has been the traditional choice, recently replaced by activated carbon, zeolites, and zirconia (ZrO_2) – the last showing high selectivity for aromatics, among oth-

ers [12, 13]. Sulphided catalysts have been found to require extra sulphur input (e.g. H_2S) to maintain activity, however, increased concentration of sulphur additives has resulted in a decrease in HDO conversion, and in supressing the hydrogenolysis route over the hydrogenation route [13].

3.3 Oxidation

3.3.1 Reaction mechanisms

Vanillin, one of the most significant lignin depolymerization products is formed by oxidation. In contrast with reduction reactions that primarily attack C-O bonds and remove moieties, oxidation techniques mainly add functionalities by cleavage of C-C bonds. Ma *et al*. [25] identify three reaction routes depending on the substrate or lignin fragment and the oxidative reagent: 1. when the phenolic molecule possesses a conjugated side chain, it is broken at the double bond to produce aldehyde, ketone, or carboxylic acid substitutions; 2. a phenolic molecule with a non-conjugated side chain may produce a quinone and/or a dicarboxylic acid by aromatic ring cleavage; 3. fragmented monomers may recombine in biphenyl structures. Complete oxidation into small compounds is also possible especially with the highly reactive ozone [25].

3.3.2 Catalysts and selectivity

Common oxidation systems studied are uncatalyzed oxidation by chlorine dioxide (ClO_2), ozone (O_3), or peroxy acids (R'COOOH) as oxidating agents, as well as catalyzed oxidation by H_2O_2 or O_2 as oxidating agents [11, 25]. Alkaline supports help to ionize the free phenolic hydroxyl groups and promote benzaldehyde/benzoic acid derivatives, while acidic supports favour extensive degradation, aromatic ring cleavage and further production of dicarboxylic acids. Alcohol addition has been reported to result in decreased fragment recondensation [25].

Catalysts resulting in enhanced selectivity towards small molecular weight aromatics in oxidation of lignin by oxygen include nitrobenzene, simple metal ions, metal oxides, polyoxometalates, and composite metal oxides [11, 25]. Werhan *et al.* [35] performed a transition metal salts catalyst screening study of kraft lignin oxidation by oxygen and found out that CoCl and $CuSO_4$ resulted in the highest

yield of target products vanillin and methyl vanillate. A study of precipitated hydrolysis lignin oxidation shows that initial high oxygen pressure is optimal for breaking the lignin molecule, followed by lower pressure to avoid further degradation of phenolic aldehydes [11].

Transition-metal catalysts are reported to accelerate degradation of H_2O_2, so earth metal compounds as well as chelating agents are suggested to stabilize the reagent and increase efficiency. Organocatalysts and organometallic catalysts including metallosalen complexes, organorhenium oxides, vanadium complexes, metal-organic frameworks (MOFs), and metalloporphyrins have been suggested for enhancing selective oxidation through side-chain conversion and selective C-O and C-C bonds cleavage. To promote selectivity towards aromatic ring cleavage and dicarboxylic acids, composite metal sulphites and organorhenium oxides are reported as suitable catalysts. [25].

3.4 Cracking

Cracking processes have been used to split hydrocarbon molecules in complex, high molecular weight fossil oil in refineries; as well as to liquefy biomass as fossil oil replacement. Unlike the previous processes, cracking applies high temperatures and from vacuum to moderate pressures in the absence of hydrolyzing, reducing or oxidizing agents.

Thermal degradation of lignin occurs through a wide range of temperatures. Results of uncatalyzed slow pyrolysis show that propanoid side chain degradation happens between 120–300 ^{0}C; the C-C interlignin linkages start to cleave at 275–350 ^{0}C and the less thermally stable aryl-ether bonds start to break at around 230 ^{0}C and disappear completely at around 375 ^{0}C. Guaiacyl type molecules are formed at lower temperatures and are followed by syringyl type molecules. Further oxidation results in catechols and derivatives with both increasing temperature and residence time. Aromatic ring cleavage and condensation lead to hydrogen release above 500 ^{0}C. These observations, however, are valid for uncatalyzed systems and shall be different for catalytic pyrolysis. [11, 36, 37].

Choi *et al*. [38] screened zeolite HZSM-5, a Fluid Catalytic Cracking (FCC) catalyst, and olivine catalyst in the fast pyrolysis of Alcell and organosolv lignin at

470 and 560 ^{0}C and concluded that the best performance in maximum oil and minimum coke yields was obtained with the HZSM-5 catalyst at both temperatures and for both Alcell and organosolv lignins; however, the maximum yield of chemicals of interest (measurable by GC/MS/FID) – benzenes, phenols, guaiacols, and syringols – was obtained using the FCC catalyst at high temperature for the Alcell lignin and the olivine catalyst at low temperature for the organosolv lignin.

EXPERIMENTAL PART

4. Experimental methodology

In the context of utilizing lignin as a source of polymers that may be broken into valuable monomeric precursors, experimental work was carried out to decompose isolated lignin, as well as to analyze properties and identify components of the product. For the catalyst screening, three experimental runs were performed and the results of each were analyzed to evaluate relative catalyst performance.

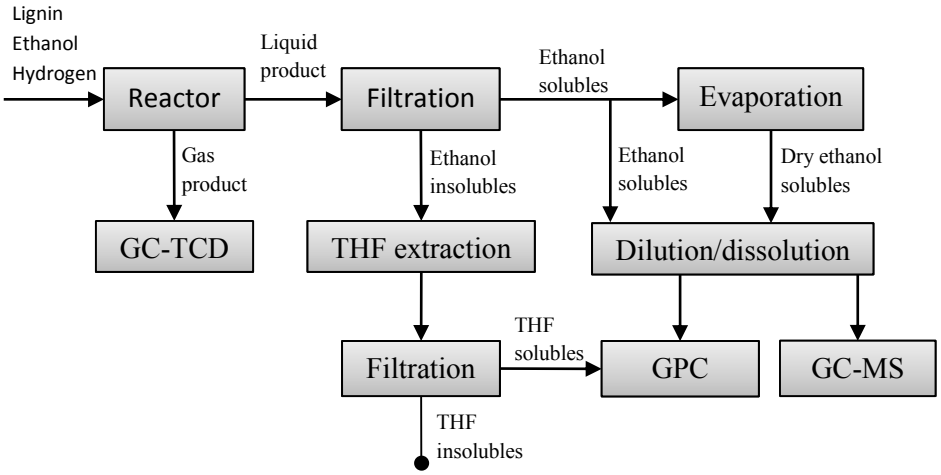

Figure 4. Experimental methodolgy schematic.

The applied experimental methodology is presented in Figure 4. Organosolv isolated lignin was added prior to the experiment to a stirred batch reactor with ethanol and hydrogen (section 4.2). After the experiment, the gas product was sampled (section 4.3.1) and analyzed (section 4.4.3) by a gas chromatograph with thermal conductivity and flame ionization detectors (GC-TCD/FID). The liquid product was recovered from the reactor after the experiment and filtrated (section 4.3.1).

From the liquid phase (ethanol solubles), aliquots were taken for 3-day open evaporation in fume hood (section 4.3.3). Samples of both fresh and 3-day evaporated liquid reaction product (ethanol solubles) were diluted in tetrahydrofuran (THF) and analyzed (section 4.4.1) by gel permeation chromatography (GPC).

Additional aliquots of the liquid reaction product (ethanol solubles) were taken for 3-day open evaporation and further dissolved in pyridine and analyzed (section 4.4.2) by gas chromatography – mass spectrometry (GC-MS).

The reaction product in solid phase (ethanol insolubles) was extracted with THF and filtrated (section 4.3.4). This liquid phase (ethanol insolubles – THF solubles) was analyzed by GPC (section 4.4.1).

Each step is described in detail in sections 4.2 through 4.4.

4.1 Feedstock acquisition

4.1.1 Lignin

The isolated lignin used for these experiments was provided by the Biorefineries research group of the Department of Forest Products Technology of Aalto University School of Chemical Technology. The organosolv lignin was obtained by extraction of beech wood with ethanol solvent by the Fraunhofer Center for Chemical-Biotechnological Processes.

4.1.2 Catalysts

Three commercial catalysts were used in the experiments. Palladium on activated carbon (Pd/C) 3 wt. % loading was purchased from *Degussa* as pellets. Pure zirconia (ZrO_2) was purchased from *MEL Chemicals* as pellets. Both catalysts were ground and sieved to $0.3 < x < 0.42$ mm particle size.

Palladium on alumina (Pd/Al_2O_3) 5 wt. % loading was purchased from *Strem* as powder. The catalyst was pelletized in an *Atlas* laboratory hydraulic press. The powder was introduced to a stainless steel round mold of 20 mm of diameter, followed by a stainless steel piston. A load of 20 tons was programmed and au-

tomatically applied through the piston in the mold. The pressure was slowly released. The results were round discs to be ground and sieved to $0.3 < x < 0.42$ mm particle size.

4.1.3 Chemicals

Hydrogen 5.0 (≥ 99.999%) and nitrogen 5.0 (≥ 99.999%) were purchased from *AGA*. Ethanol (≥ 99.5%) was purchased from *Altia*. THF (≥ 99.9%) and pyridine (≥ 99.5%) were purchased from *Merck*.

4.2 Hydrodeoxygenation reaction

4.2.1 Preparation

The lignin was gently crushed using a mace and a mortar, and checked thoroughly to avoid agglomeration. For each reaction, 50 ml of ethanol, 0.1 g of catalyst, and 1 g of lignin were used.

4.2.2 Experiments

The experiments were performed in a stirred high pressure / high temperature 100 ml batch reactor of Hastelloy C-276 alloy – rated at 345 bar, 500 °C – component of a commercial Parr system (model 4598). The vessel was tightened through a graphite gasket by split rings with cap screws. The system included PID controllers for pressure, temperature, and stirrer speed.

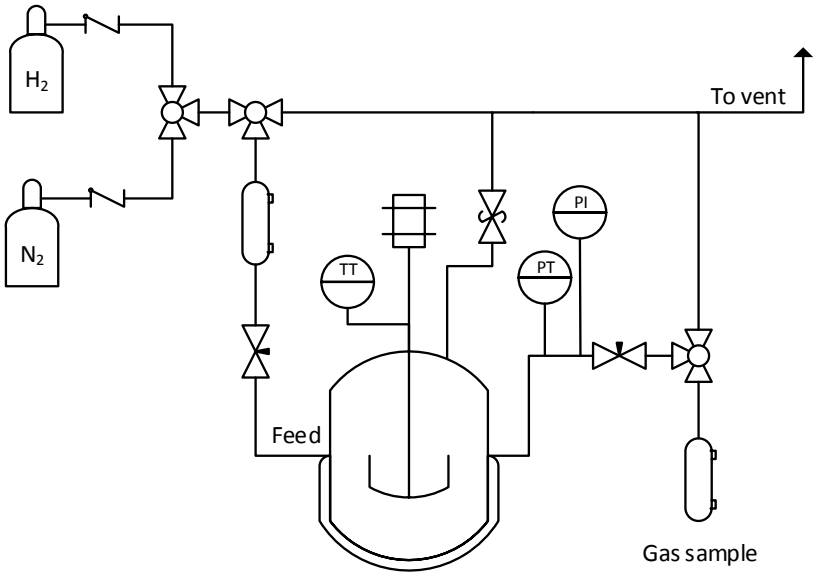

Figure 5. Reactor schematic.

The lignin and ethanol were loaded into the reactor vessel, and the catalyst was loaded into a stirrer equipped with four 0.25 mm mesh baskets, custom-made by the workshop of Aalto University School of Chemical Technology. The reactor was purged three times with 10 barg nitrogen and a pressure test was performed at 100 barg. The system was purged three times with 10 barg hydrogen and pressurized to the desired cold pressure, followed by controlled heating to the desired temperature setpoint. The reaction time of all experiments was 1 hour, and the stirring speed was 1000 rpm.

The reaction was stopped by removing the heating jacket and applying pressurized air to the reactor surface, followed by a room temperature water bath enclosing the reactor vessel. The system was left stirred at 200 rpm overnight for further cooling to room temperature (24–25 °C).

4.2.3 Washing

After product recovery and treatment, the reactor vessel and stirrer were washed with acetone. The reactor system was purged with 10 barg nitrogen three times to remove any gas product from the lines. The system was pressure tested at 50 barg, vented, and ran with ethanol at 200 °C and 200 rpm stirring for 30 minutes.

4.3 Product treatment

In section 4.2 was described how the experiments were performed. The reaction product consisted of a gas, a liquid, and a solid phase. The product recovery and separation between the liquid and solid reaction products is shown in Figure 6.

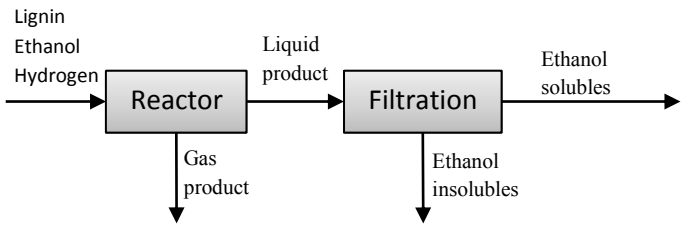

Figure 6. Schematic of the product recovery and filtration methodology.

4.3.1 Product recovery

After overnight cooling, the water bath was removed. A gas sampling container of 5.9 ml was emptied in vacuum for 10 min. In the reactor system, the sampling line (bottom right section of Figure 5) was flushed with the gas product by slowly and partially venting said line (except the last section, containing an estimated volume of 3.6 ml of air). Then, the gas sampling container was connected and filled. After the gas sample was taken, all the gas product was vented, including that inside the sampling line. The gas sample was analyzed by GC-TCD (section 4.4.3).

The liquid product was recovered with the aid of 25 ml of ethanol total, and then vacuum-filtrated. The reactor stirrer was washed with 2.5 ml of ethanol and left to dry overnight in a fume hood. The recovery procedure was done in a fume hood. It consisted first on transferring the liquid phase from the reactor vessel to a screw-cap glass bottle with a pipette equipped with a plastic disposable tip. Most of the solids were transferred to the same bottle with a metal spatula. 5 ml of ethanol were added to the reactor vessel and the mix (ethanol and small solid particles) was transferred with the pipette to the product glass bottle. The procedure was repeated until the 25 ml of ethanol wash were finished. The treatment of ethanol insolubles trapped in the reactor vessel are described in section 4.3.4.

4.3.2 Filtration of ethanol solubles

The filtration was done in vacuum through a grade GF/A glass microfiber round filter of 70 mm (diameter) in a Büchner funnel and flask. The liquid product was transferred to the Büchner flask with the pipette. Most of the solid was transferred to the glass microfiber filter with a spatula. 5 ml ethanol were added to the liquid product container and the mix (ethanol and small solid particles) was transferred with the pipette to the Büchner flask. Finally, the solids in the microfiber filter were washed with 5 ml ethanol. As result are three product treatment streams as presented in Figure 6: ethanol solubles, ethanol insolubles, and gas product.

4.3.3 Ethanol solubles treatment

The treatment of the ethanol solubles part of reaction products was divided in two analyses: GPC and GC-MS, as shown in Figure 7.

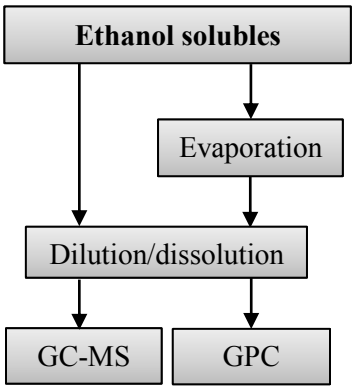

Figure 7. Schematic of product treatment of ethanol solubles.

Gel permeation chromatography

Two aliquots of 0.5 g of filtrate were drawn for 3-day open evaporation in a fume hood. After 3 days, they were weighed and dissolved in THF. Two fresh filtrate samples were drawn and diluted in THF as well. These four samples were pre-

pared in concentrations between 2–3 mg bio-oil per 1 ml THF, injected through 0.45 µm filters and analyzed by GPC (section 4.4.1).

Gas chromatography – mass spectrometry

Three aliquots of 0.3 g of filtrate were drawn – injected through 0.2 µm pore size filters – for 3-day open evaporation in a fume hood The three dry microfiltrated samples were dissolved in 100 µl of cumene-pyridine (0.075 wt. %) and 300 µl of pyridine. These three samples were analyzed by GC-MS (section 4.4.2).

4.3.4 Ethanol insolubles treatment

The treatment of ethanol insolubles consists of extraction with THF and filtration, resulting in a residue to be analyzed by GPC, and char, as shown in Figure 8.

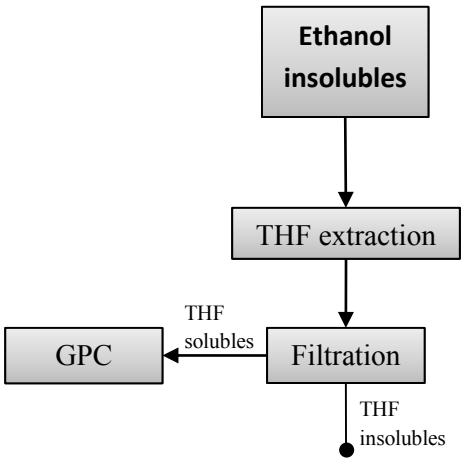

Figure 8. Schematic of product treatment of ethanol insolubles.

Extraction

The filter with ethanol insolubles was extracted with 40 ml of THF total. Halfway inside a glass bottle, the filter was washed with 5 ml of THF two times. Turned upside down, the filter was washed again with 5 ml of THF two times. The filter

was then submerged into the extract and washed for a few seconds. The filter was taken halfway out and washed with 5 ml THF four times.

The insolubles on the reactor vessel were extracted with 5–10 ml of THF and transferred to the extract container. The extract was stirred for 2 hours with the reactor agitator inside to extract the solids on its surface.

Filtration and analysis preparation

The filtration was done in vacuum through a grade GF/A glass microfiber round filter of 70 mm (diameter) in a Büchner funnel and flask. The liquid product was transferred to the Büchner flask with the pipette. Most of the solid was transferred to the glass microfiber filter with a spatula. 2.5 ml THF were added to the liquid product container and the mix (THF and small solid particles) was transferred with the pipette to the Büchner flask. Finally, the solids in the microfiber filter were washed with 2.5 ml THF.

The THF solubles filtrate was left for open evaporation overnight in a fume hood, and the next day a microfiltrated sample (0.45 µm pore size) was analyzed by GPC (section 4.4.1).

4.4 Analyses

All mass quantities were weighed in an analytical scale with readability to 0.1 mg (mainly Precisa 185AM-FR). Liquids were handled with a 5 ml Finnpipette and plastic disposable tips.

4.4.1 Gel permeation chromatography

Molecular weight analysis of the reaction products was performed by gel permeation tography (GPC) and variable wavelength detection (VWD). The array was based on an *Agilent* 1100 Series high performance liquid chromatography (HPLC) system including a quaternary pump, vacuum degasser, autosampler, and variable wavelength detector (VWD).

Two Phenogel size exclusion columns by *Phenomenex* were used, both 300 mm length by 7.8 mm internal diameter, of cross-linked styrene-divinylbenzene stationary phase, 5 µm particle size, one with 100 and the other with 1000 Å pore size. A Phenogel guard column by *Phenomenex* was also used, of 50 mm length and 7.8 mm internal diameter, of coss-linked styrene-divinylbenzene, 5 µm particle size.

The analyses were conducted with an eluent (THF) flow of 1 ml/min, a 50 µl injection volume, and a column pressure of 43.5 ± 0.2 barg. Detection was carried out at 280 nm wavelength, which has been mentioned as the wavelength of maximum absorption for species of hardwood [39]. The equipment was controlled through the OpenLAB CDS ChemStation software provided by *Agilent*. Calibration, data analysis and calculations were done through the ChemStation GPC Data Analysis Sofware addon provided by *Agilent*.

A calibration curve was constructed by two standard solutions containing toluene, syringol, 2,2'-dihydroxybiphenyl, and polystyrenes of molecular weights 208, 474, 1270, 3470, 7000, 18200, and 76600 g/mol. The curve was fitted as a 5^{th} degree polynomial. Each analysis run the standards were checked and if necessary, the curve was adjusted with a tolerance criterion of 0.04 min of retention time shift.

Two molecular weight averages were calculated. The number average (M_n) is the statistical average molecular weight of all chains, and was calculated with equation (1). The weight average (M_w) includes the contribution of each chain to the molecular weight average, and was calculated with equation (2). The polydispersity index is used to measure the heterogeneity of molecular weights, or how wide the molecular weight distribution is, and was calculated with equation (3).

$$M_n = \frac{\sum N_i M_i}{\sum N_i} \tag{1}$$

$$M_w = \frac{\sum N_i {M_i}^2}{\sum N_i M_i} \tag{2}$$

$$PDI = \frac{M_w}{M_n} \quad (3)$$

where M_n is the number average molecular weight
M_w is the weight average molecular weight
M_i is the molecular weight of a chain
N_i is the number of chains of that molecular weight

For the calculation of the molecular weight averages, the distribution, and the polydispersity index (PDI) of each sample, each chromatogram was integrated from 10 to 23.5 minutes of retention time. The integration range is based on the results of the standard solutions, in which the detector response minimum before the first compound (polystyrene of 76600 g/mol) elutes is 10.3 min, and the detector response minimum after the last compound (toluene) elutes is 23.3 min. The chromatogram of the standard solutions can be found in Appendix 1 and 2.

In order to further characterize the liquid reaction product, a criterion was defined to divide the samples into light compounds fraction (monomers and dimers) and heavy compounds fraction (trimers and further bigger oligomers). The division was made at 19.2 minutes of retention time, which, based on the results of the standard solution, is the minimum of detector response between the elution peaks of the trimer in polystyrene of 474 g/mol and 2,2'-dihydroxybiphenyl.

4.4.2 Gas chromatography – mass spectrometry

Light compound indentification was performed by GC-MS. The array was based on an *Agilent* 7890A GC platform and 5975C MS detector including an autosampler. An *Agilent* HP-5 column of (5%-Phenyl)-methylpolysiloxane stationary phase was used with dimensions of 30 m length, 0.25 mm internal diameter, and 0.25 µm film thickness.

The injection method consisted of acetone and pyridine wash, followed by a 1 µl sample injection volume through an inlet temperature of 280 °C. The sample was fed with helium at 17.5 ml/min with a 25:1 split ratio. The oven program started at 40 °C, with 5 °C/min increase to 300 °C, kept for 3 minutes. The MS

technique was electron impact ionization (EI). The electron energy parameter was 70 eV, and the scan range was from 30 to 400 amu.

4.4.3 Gas chromatography – thermal conductivity detection

Reaction gas product identification was done by GC-TCD/FID in an *Agilent* 6890N network GC system. Two capillary columns were used. An *Agilent* HP-PLOT Q of bonded polystyrene-divinylbenzene column of 30 m length, 0.53 mm internal diameter and 40 µm film thickness was followed by an *Agilent* HP-PLOT MS of 5 Å molecular sieve with dimensions of 30 m length, 0.53 mm internal diameter and 25 µm film thickness.

The oven program started at 40 °C for 9.50 minutes, followed by an increase rate of 10 °C/min to 200 °C. The sample was manually injected with 5% methane in argon carrier gas. Detection in TCD was done at 250 °C with reference flow of 20 ml/min and makeup nitrogen flow of 5 ml/min. A calibration curve was constructed for carbon dioxide, hydrogen, carbon monoxide and methane.

5. Experimental results

The experimental work consisted of catalyst screening. Three experimental runs were performed and the results of each compared to evaluate relative catalyst performance. The feedstock quantities and reaction parameters were kept constant so that the only variable was the catalyst used. In Table 2, the experimental conditions of all experiments are presented. The nomenclature for each experimental run is based on the catalyst used.

Table 2. Summary of experimental conditions. The nomenclature for each run is based on the catalyst used.

	Pd/C 3%	ZrO2	Pd/Al2O3 5%
Feedstock			
Lignin (g)	0.9885	0.9905	0.9933
Catalyst (g)	0.0973	0.1005	0.1001
Catalyst particle size (mm)	0.3<x<0,42	0.3<x<0.4	0.3<x<0.42
Ethanol (g)	39.112	39.1226	39.2277
Reaction			
Initial hydrogen pressure (barg)	46	47.8	46.5
Temperature setpoint (°C)	300	300	300
Reaction time (minutes)	60	60	60
Stirring speed (rpm)	1000	1000	1000
Final hydrogen cold pressure (barg)	44.1	47.1	45.9
Final cold temperature (°C)	23	23	24

5.1 Yields and solubility characteristics

As mentioned in the description of the experimental methodology, the gas product was vented, while the liquid product was filtrated and the ethanol insolubles were extracted with THF. This resulted in two organic fractions, ethanol solubles and ethanol insolubles (THF solubles). For the purposes of presentation of results, these fractions are named light bio-oil and heavy bio-oil, respectively.

Table 3. Absolute mass yields (dry) for all experimental runs normalized with respect to amount of lignin feedstock.

	Pd/C 3%	ZrO2	Pd/Al2O3 5%
Lignin feedstock	0.9885	0.9905	0.9933
Ethanol solubles (light bio-oil)	0.6489	0.6705	0.7689
THF solubles (heavy bio-oil)	0.0294	0.0193	0.0171
THF insolubles (char)	0.1228	0.1521	0.1727

In Table 3, mass yields of the ethanol-soluble "light bio-oil" fraction, the ethanol-insoluble but THF-soluble "heavy bio-oil" fraction, and the THF insolubles, denominated char, normalized with respect to amount of lignin feedstock, are presented. In regards to yield of light bio-oil, the experiment involving Pd/Al_2O_3 exhibited the best performance.

5.2 Gas product analysis

Analysis of the gas product was performed to quantify the calibrated gases carbon dioxide, hydrogen, carbon monoxide, and methane.

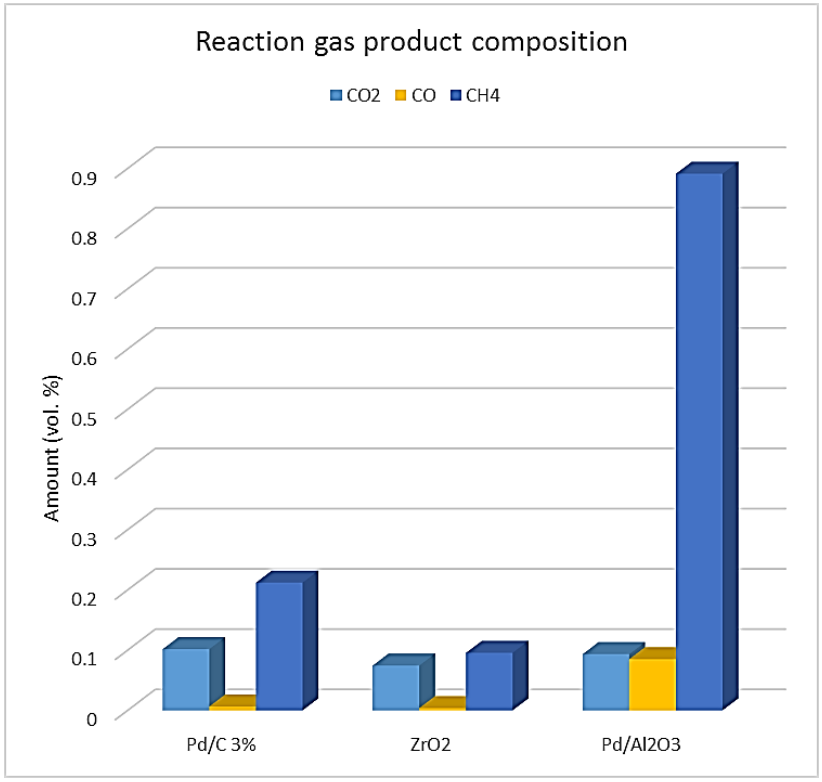

Figure 9. Partial composition of the recation gas product (CO_2, CO, and CH_4) for all experimental runs.

In Figure 9, a partial composition – only regarding carbon dioxide, carbon monoxide, and methane – for the hydrodeoxygenation reaction gas product is presented for all the experimental runs. The highest differences in the results concerns primarily methane and less carbon monoxide. The methane and carbon dioxide contents of the gas product for the experiment involving the Pd/Al_2O_3 5% catalyst are as high as 8.3 times and 21.1 times, respectively, than those of the experiment involving the ZrO_2 catalyst.

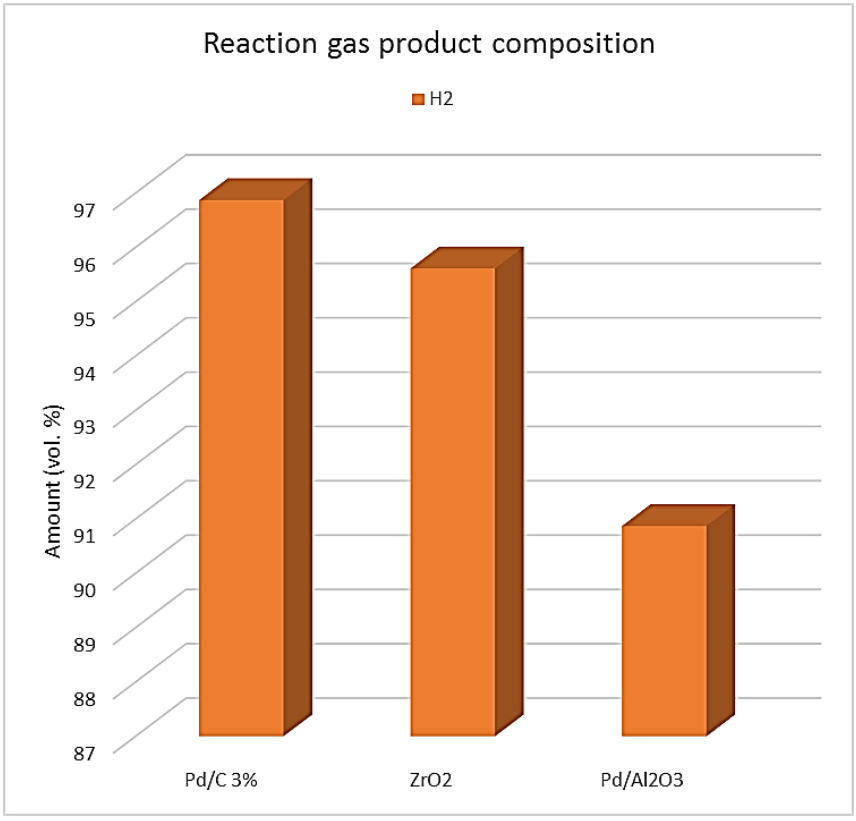

Figure 10. Hydrogen concentration of reaction gas product for all experimental runs.

In Figure 10 the concentration of hydrogen in the hydrodeoxygenation reaction gas product is shown for all experimental runs. The highest concentration corresponds to the experiment involving the Pd/C 3% catalyst, followed by that involving the ZrO_2 catalyst, the lowest being for that involving the Pd/Al_2O_3 5% catalyst. Comparing the results of the Pd/Al_2O_3 5% catalyst experiment from Figures 9 and 10, the decrease in hydrogen and increase in methane could be attributed to a higher hydrogenation activity of the catalyst, resulting in severe fractionation of the aromatic side chains, including methyl substitutions.

5.3 Liquid product properties and composition

In order to describe the properties and composition of the whole product, including its components non-identifiable by GC-MS, the liquid product was analyzed by GPC. The results presented in this section are divided by characteristics of product bio-oil fractions (light bio-oil vs. heavy bio-oil) and effect of evaporation (bio-oil in solvent vs. dry). Furthermore, the performance of different catalysts is compared.

5.3.1 Characteristics of bio-oil fractions

Average molecular weight

Before comparing the performance of the different catalysts (section 5.3.3), the different properties resulting from GPC analysis are introduced and compared in this subsection.

The liquid product properties resulting from GPC analysis are shown in Tables 4–6. Four parameters are considered in this section: number-average molecular weight, weight-average molecular weight, polydispersity index (PDI), and the custom-defined fraction of light and heavy compounds. Where the fraction of light compounds is based on the integrated area percent of detector response before and after 19.2 min of elution time – minimum of detector response between the elution peaks of the trimer in polystyrene of 474 g/mol and 2,2'-dihydroxybiphenyl. In other words, fraction of – assumed – monomers and dimers.

Table 4. Molecular weight averages and PDI of the light bio-oil product fraction in solvent.

Light bio-oil				
Unit	**Variable**	**Pd/C 3%**	**ZrO_2**	**Pd/Al_2O_3 5%**
(g/mol)	**Mn**	363.4	374.3	432.1
	Mw	583.9	609.6	677.9
	PDI	1.607	1.629	1.569
	Light compounds fraction	0.24047	0.2344	0.15305

Table 5. Molecular weight averages and PDI of the evaporated light bio-oil product fraction

Evaporated light bio-oil				
Unit	**Variable**	**Pd/C 3%**	**ZrO_2**	**Pd/Al_2O_3 5%**
(g/mol)	**Mn**	380.2	401.5	444.8
	Mw	633.9	716.4	741.2
	PDI	1.667	1.784	1.666
	Light compounds fraction	0.22144	0.20791	0.14627

Table 6. Molecular weight averages and PDI of the heavy bio-oil product fraction.

Heavy bio-oil				
Unit	**Variable**	**Pd/C 3%**	**ZrO_2**	**Pd/Al_2O_3 5%**
(g/mol)	**Mn**	1207	918.6	973.6
	Mw	3133	2808	2845
	PDI	2.594	3.057	2.922
	Light compounds fraction	0.02938	0.04677	0.03655

In order to compare the results with ease, comparisons of each parameter for the light- and heavy- bio-oil product fractions are shown in Figures 11–13.

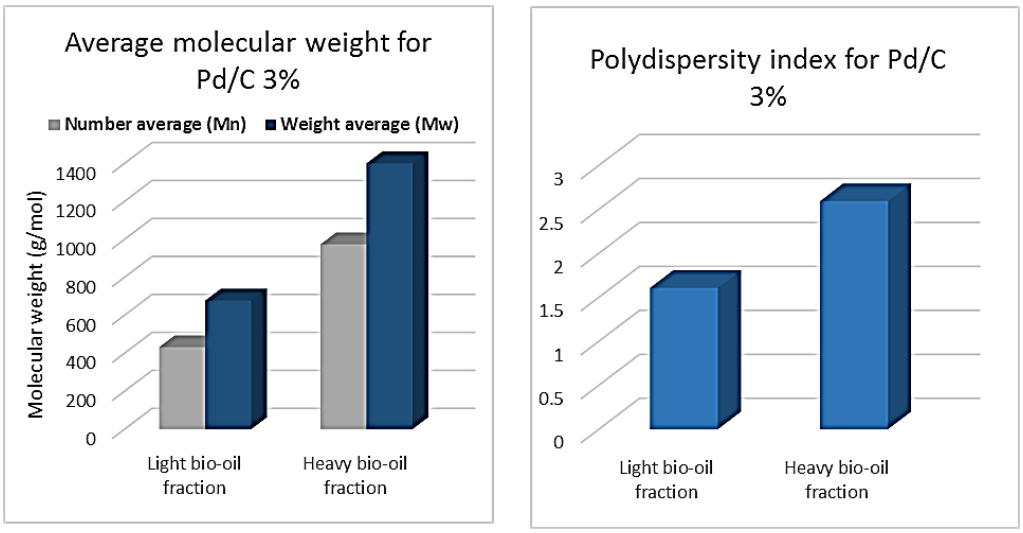

Figure 11. Comparison of the number and weight average molecular weights and PDI for the light and heavy bio-oil fractions for the experiment involving the Pd/C 3% catalyst.

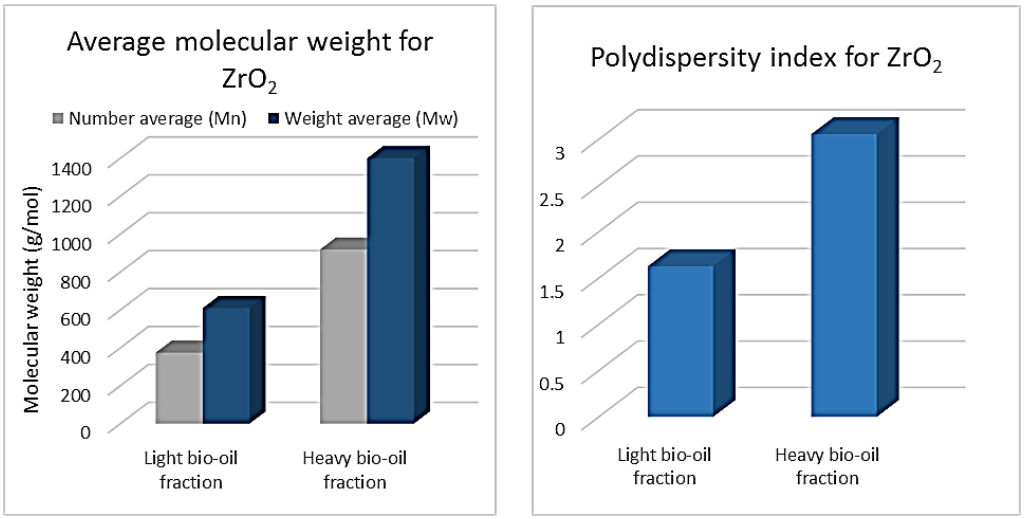

Figure 12. Comparison of the number and weight average molecular weights and PDI for the light and heavy bio-oil fractions for the experiment involving the ZrO_2 catalyst.

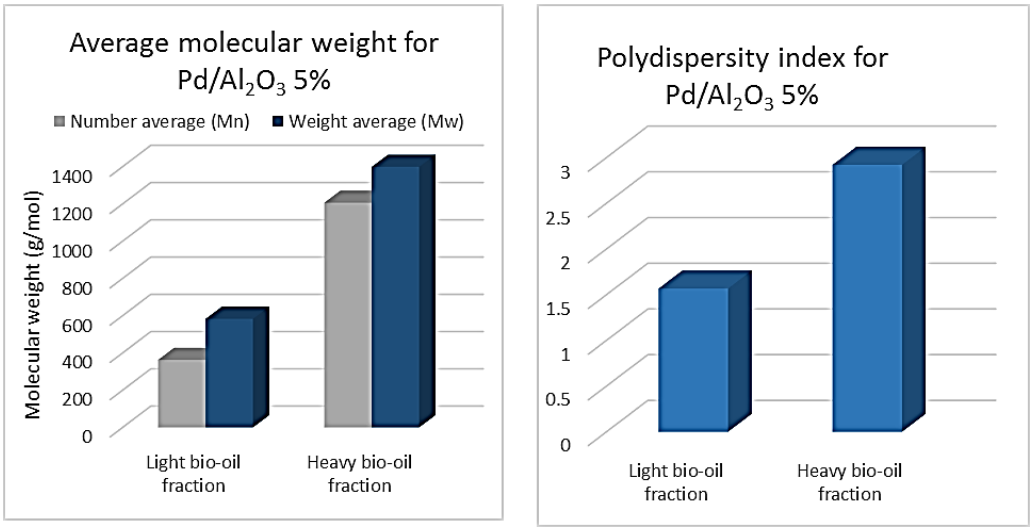

Figure 13. Comparison of the number and weight average molecular weights and PDI for the light and heavy bio-oil fractions for the experiment involving the Pd/Al_2O_3 5% catalyst.

Figures 11–13 show an increase of molecular weight from the light to the heavy bio-oil fractions for all experiments. As the latter contains the compounds that were insoluble in ethanol but soluble in THF, it may be concluded that the light bio-oil (ethanol soluble fraction) is more relevant for the purpose of isolating small molecular weight compounds. Furthermore, even if the considerably high molecular weight average of the heavy bio-oil fraction signifies the need for further decomposition, the mass balance in Table 3 shows it represents less than 5% the amount of light bio-oil for all runs.

The difference between the number average and weight average molecular weights is bigger in the heavy bio-oil fraction, as shown in the PDI of all experiments. A higher PDI means a wider distribution, a wide range of different molecules that may represent a need for separation. Additionally, higher molecular weight differences suggests high differences in boiling points, opening the possibility to separation by distillation. A lower PDI for the light bio-oil fraction may be seen as a good result in the perspective of future chemical treatment for direct applications [40]. The higher polydispersity might be attributed to a non-uniform depolymerization process [41].

Molecular weight distribution

Aside from the molecular weight averages, the molecular weight distribution is useful for understanding the rough composition of a substance.

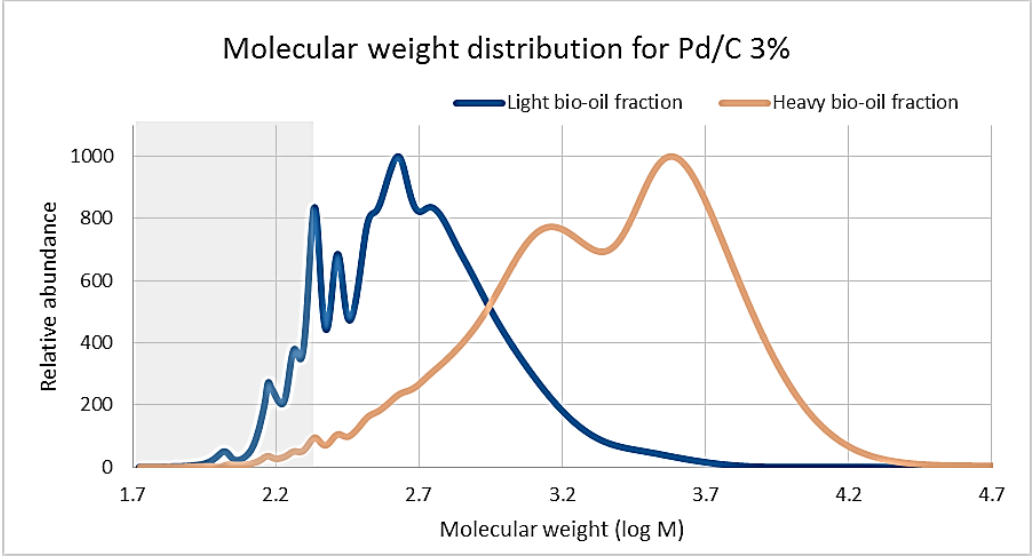

Figure 14. Molecular weight distribution for both the light bio-oil and heavy bio-oil fractions for the experiment involving the Pd/C 3% catalyst.

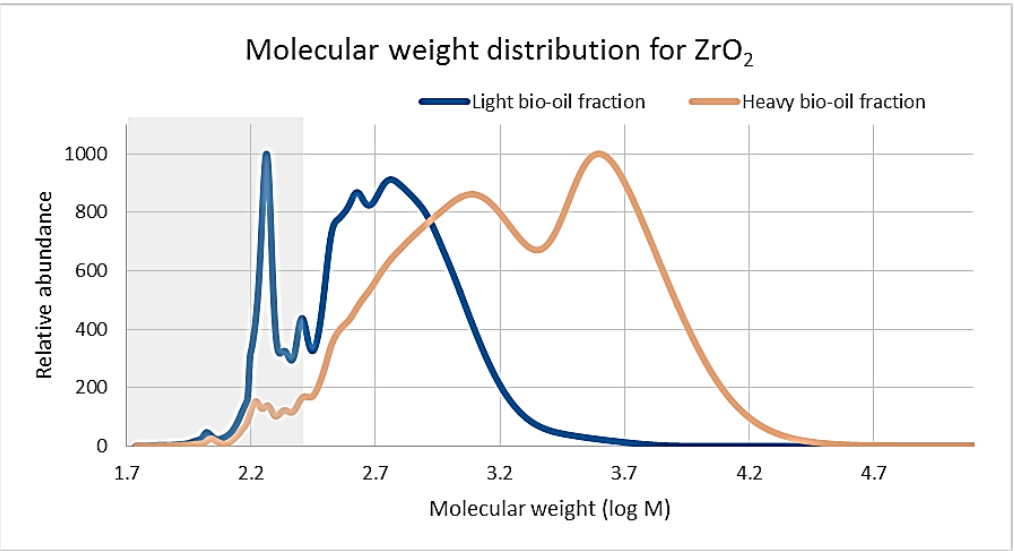

Figure 15. Molecular weight distribution for both the light bio-oil and heavy bio-oil fractions for the experi-ment involving the ZrO_2 catalyst.

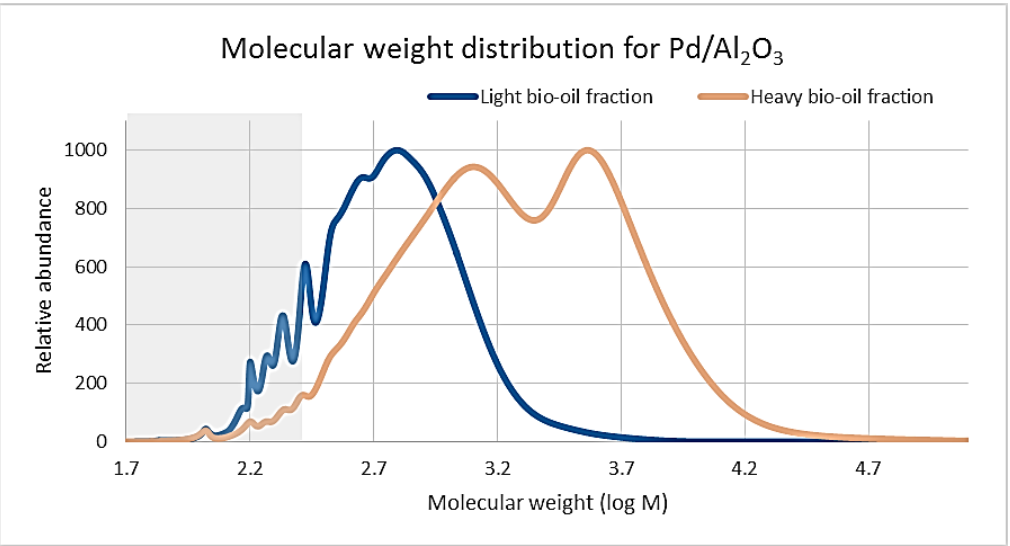

Figure 16. Molecular weight distribution for both the light bio-oil and heavy bio-oil fractions for the experi-ment involving the Pd/Al_2O_3 5% catalyst.

Figures 14–16 show the molecular weght distribution of both the ligh bio-oil fraction and the heavy bio-oil fraction for each experiment. For improving the comparison between the bio-oil fractions, all of the distributions were scaled so that the maximum relative abundance value for each function was 1000 units. As mentioned above, the PDI of the heavy bio-oil fraction is higher, representing a wider distribution. This can also be observed by the shape of the distributions.

It's worth noticing the overlap between the profiles of both fractions. It can be appreciated that there's a considerable amount of relatively lower molecular weight molecules in the heavy fraction. This may be attributed to deficiency in the filtration, as some ethanol solubles carried out with the insolubles that were afterward extracted with THF.

Another notable shared characteristic between all the experiments is the clear bimodal molecular weight distribution of the heavy bio-oil fraction. This behaviour in which there are two predominant groups of molecules with similar molecular weights may represent ease of separation of at least these two segments, for example by solvent-non-solvent fractionation or by vacuum distillation [42].

An added aspect in figures 14–16 is a shaded section in the left side. This section represents a custom-defined calculation of light (monomers and dimers) and heavy (trimers and heavier oligomers) compounds. It can be observed that the portion of light compounds in the heavy bio-oil fraction is relatively small. This can also be observed in figures 17 and 18.

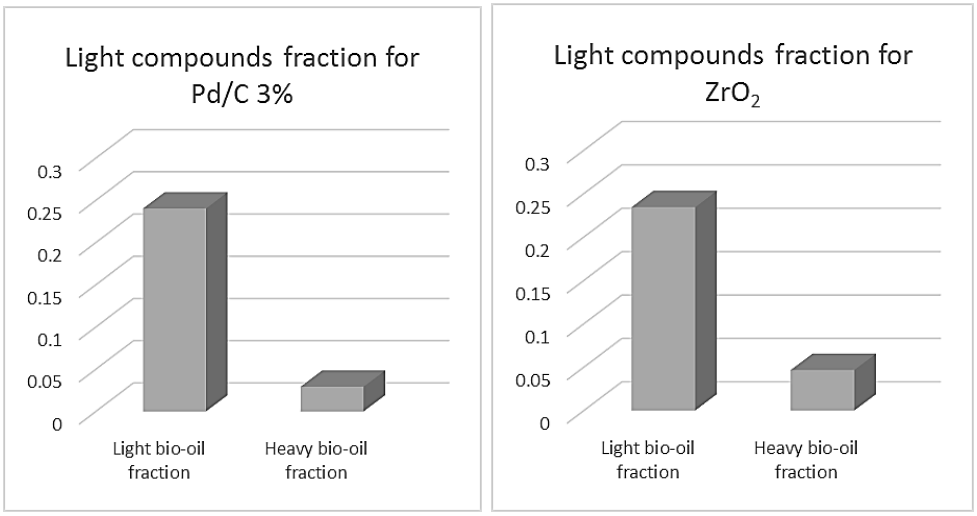

Figure 17. Comparison of the custom-defined light compounds fraction for the light and heavy bio-oil fractions for the experiments involving the Pd/C 3% and ZrO_2 catalysts.

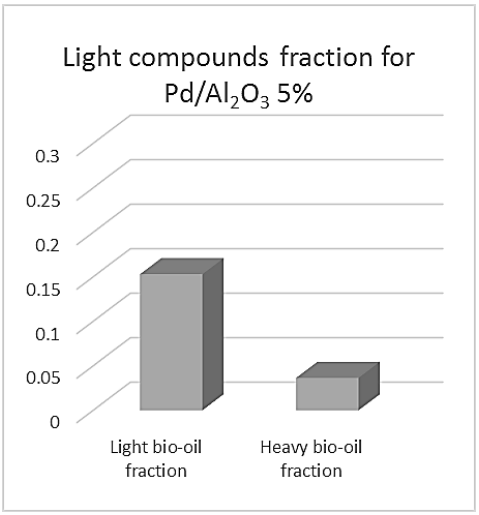

Figure 18. Comparison of the custom-defined light compounds fraction for the light and heavy bio-oil fractions for the experiment involving the Pd/Al2O3 5% catalyst.

Figures 17 and 18 show a comparison of the custom-defined light compounds fraction for the light and heavy bio-oil fractions for all experiments. As mentioned above for the molecular weight distribution profiles, the light compounds fraction is considerably higher in the light bio-oil fraction, less for the experiment involving the Pd/Al_2O_3 catalyst. Still, the presence of light compounds in the heavy bio-oil fraction may represent a need for improvement in the experimental methodology and minimization of human error regarding filtration.

5.3.2 Effect of evaporation

All the results presented in the previous sub-section for the light bio-oil fraction of the hydrodeoxygenation reaction product were based on samples with original solvent – ethanol – and presumably water generated in the reaction. When the samples were evaporated, the changes in their characteristics are presented next.

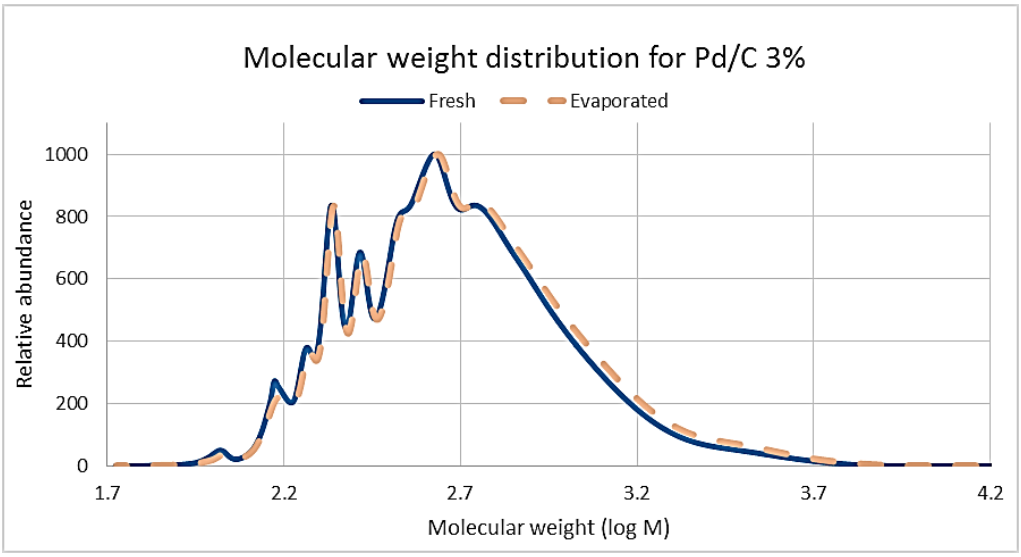

Figure 19. Molecular weight distribution for the light bio-oil fraction fresh from the reactor and after 3 days of open evaporation for the experiment involving the Pd/C 3% catalyst.

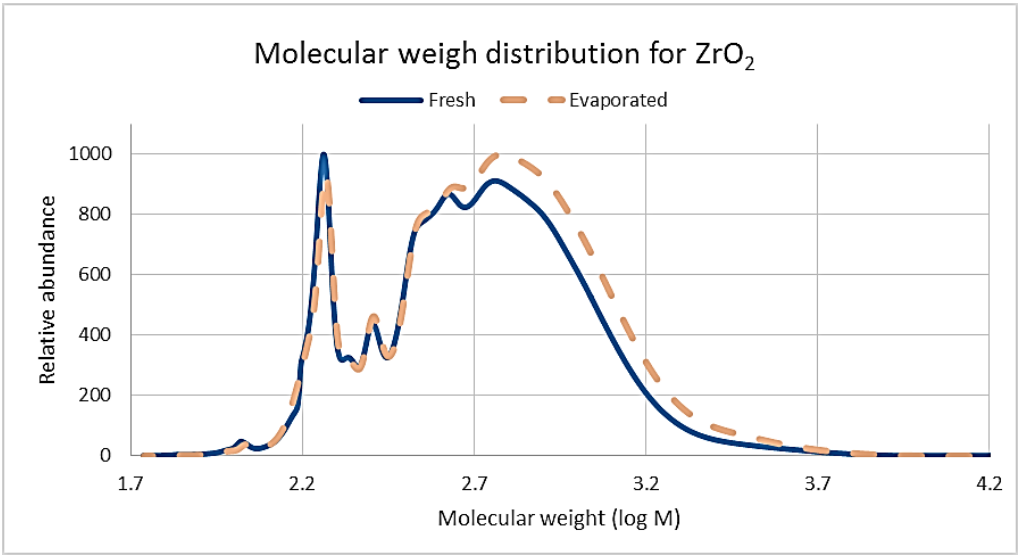

Figure 20. Molecular weight distribution for the light bio-oil fraction fresh from the reactor and after 3 days of open evaporation for the experiment involving the ZrO_2 catalyst.

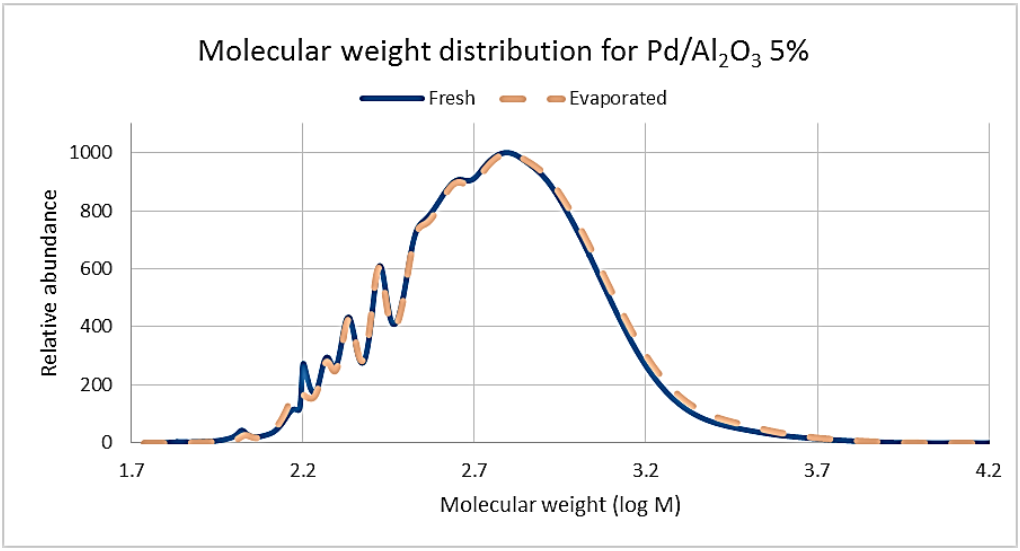

Figure 21. Molecular weight distribution for the light bio-oil fraction fresh from the reactor and after 3 days of open evaporation for the experiment involving the Pd/Al_2O_3 5% catalyst.

Figures 19–21 show the molecular weight distribution of the light bio-oil fraction for samples of both fresh reactor product and after 3-day open evaporation for all experiments. The trends for both samples in each experimental run are similar, however, the function of the evaporated sample is shifted slightly towards a higher molecular weight, most prominently for the experiment involving the ZrO_2 catalyst. This shift in distribution may be attributed to evaporation of small molecular weight volatiles, including potentially valuable aromatics. The differences in molecular weight averages are better observed in Figure 22. There's also a considerable change in polydispersity (distribution width), especially for the ZrO_2 experiment, that is better appreciated in the PDI comparison in Figure 22.

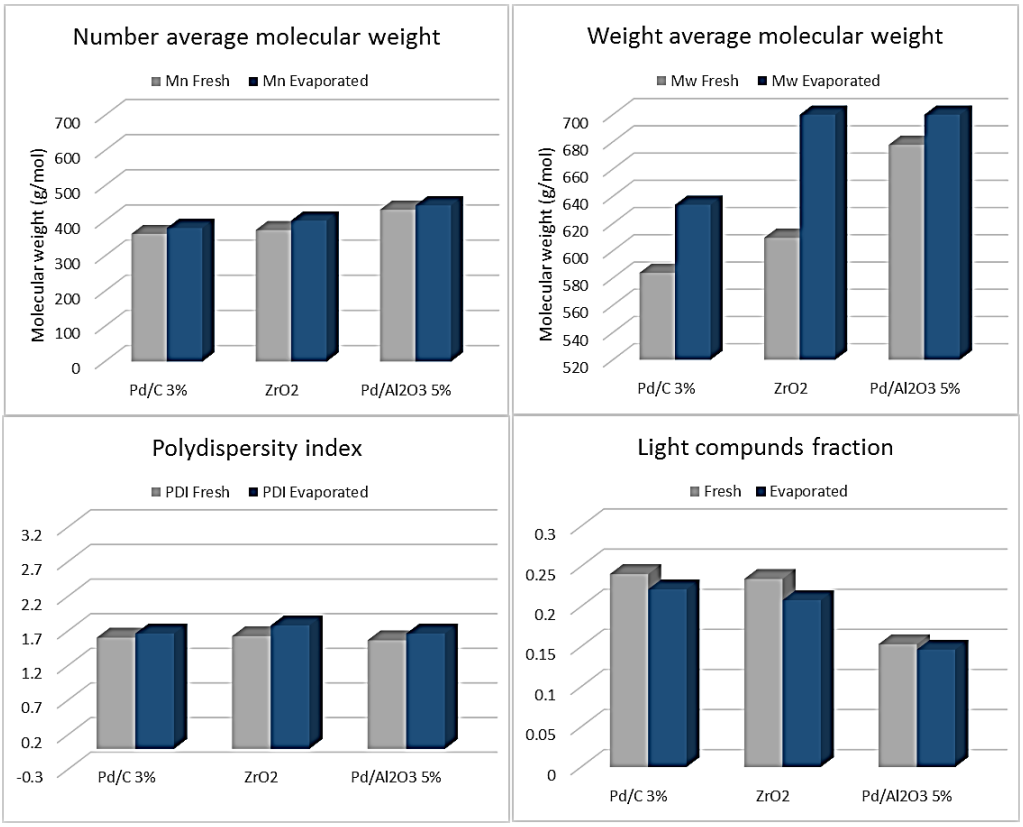

Figure 22. Comparison of molecular weight characteristics of light bio-oil as fresh reaction product and after 3-day open evaporation, and for each experiment.

Figure 22 shows a comparison of four characteristics of the fresh reaction product sample, and after 3 days of open evaporation. Simultaneously, all the experiments are compared. From observing the top sections (the number- and weight-average molecular weights), there does not appear to be a correlation between shift in molecular weight average and its value, because centering in the experiment involving the ZrO_2 catalyst, the lower molecular weight sample (Pd/C 3%) has more shift than the higher molecular weight average sample (Pd/Al_2O_3) but still both have less shift than the ZrO_2 experimental run. The same lack of correlation is shown as well in the bottom right graph (of custom-defined light compounds fraction). In regards to the criteria of minimum loss of product in evaporation, Pd/Al_2O_3 displays the best performance.

An interesting change between fresh and evaporated samples is that of the PDI. If light compounds are evaporated and lost, the range of molecular weight should decrease. However, an increase in polydispersity suggests a rearrange-

ment of molecules, in other words, the product either reacts with oxygen as it evaporates over time and/or it recombines and oligomerizes at room temperature.

5.3.3 Catalyst screening

As mentioned in the previous section, the light bio-oil fraction is more relevant for analysis of small molecular weight aromatics. The comparisons of the molecular weight distribution, number- and weight-average molecular weight, polydispersity, and custom-defined light compounds fraction for the light-bio-oil product fraction are presented below for all experiments.

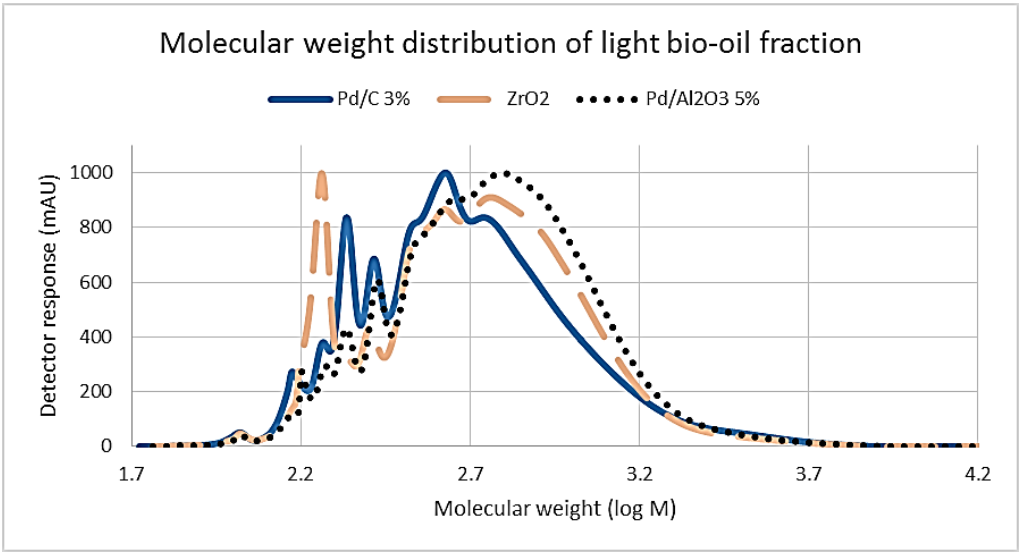

Figure 23. Molecular weight distribution for the light bio-oil fraction for all experiments.

In Figure 23 a comparison of the molecular weight distribution for the light bio-oil product fraction for all experiments is shown. It can be observed that the function of the experiment involving the Pd/C 3% catalyst is the leftmost centered, therefore containing lower molecular weight molecules in average. The experiment involving the Pd/Al_2O_3 is in the contrary encompassing the highest molecular weight molecules of the experimental runs. It can also be seen that the widest distribution and polypersity belongs to the experiment involving the ZrO_2 catalyst, representing more potential difficulty for further chemical treatment for direct applications, but higher ease for separation based on boiling point difference.

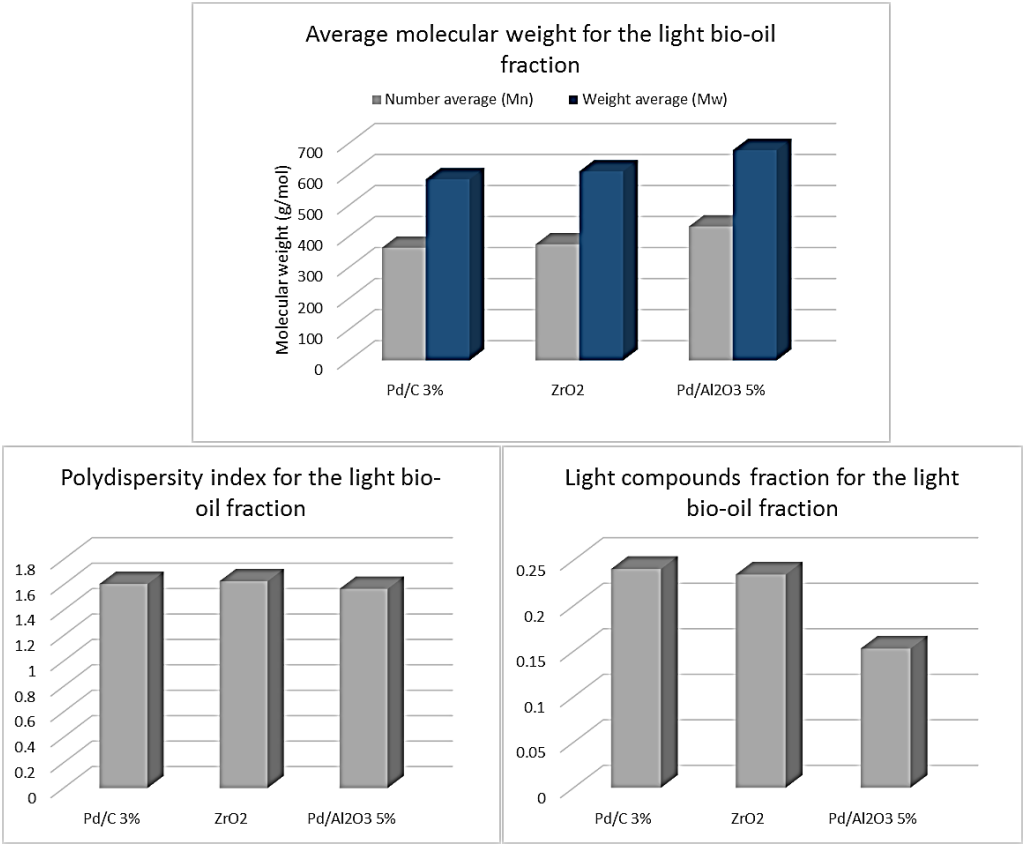

Figure 24. Average molecular weight, polydispersity index, and light compounds fraction for the light bio-oil fraction for all experiments.

In Figure 24 the comparison of the number- and weight-average molecular weight, polydispersity, and light compounds fraction is shown for the light bio-oil product fraction for all experiments. Regarding the average molecular weight, the experiment involving the Pd/C 3% catalyst had the best performance with the lowest values: 363.4 g/mol of number average and 583.9 g/mol of weight average. The best result for fraction of light compounds also belongs to the Pd/C catalysed experiment, with the value of 24.1%. In the polydispersity criteria, the Pd/Al_2O_3 catalyzed experiment had the best outcome, with the lowest value of PDI.

5.4 Identification of compounds

Aside from determination of the molecular weight distribution and properties of the liquid reaction product, light compounds were identified by GC-MS.

Table 7. Identified and suggested compounds compounds and their source of identification: standard solution, NIST database with Match Factor (%), and/or literature.

		Identification	
Compound	**Molecule**	**NIST Match Factor (%)**	**STD / Literature**
Guaiacol	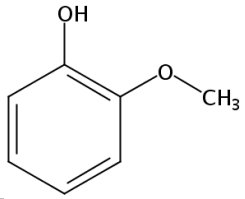	92.8	STD solution, [43]
4-Methylguaiacol	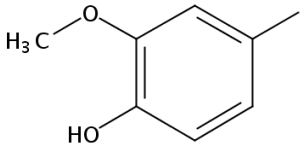	96.0	STD solution, [43]
Vanillin	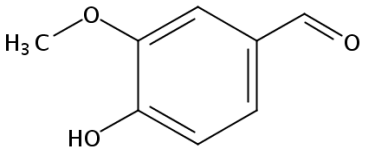	88.5	STD solution, [43]
4-Ethylguaiacol	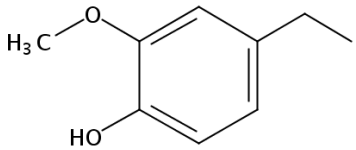	94.0	STD solution, [43]
Syringol	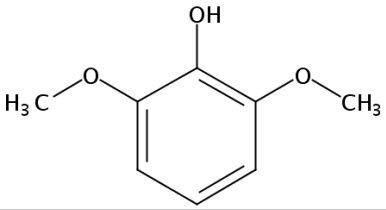	98.9	STD solution, [43]
Eugenol	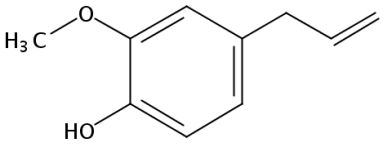	83.4	[43]
***trans*-Isoeugenol**	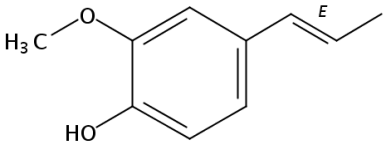	-	STD solution, [43]

Acetovanillone	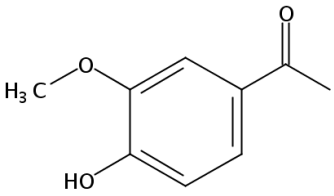	85.9	[43]
4-Propylguaiacol	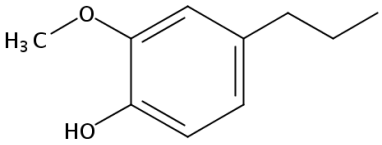	93.1	Standard solution, [43]
4-methylsyringol	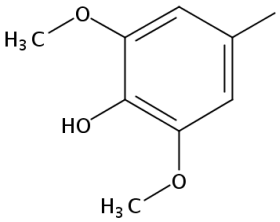	-	[43]
Guaiacylacetone	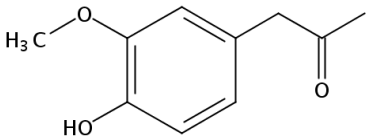	78.6	[43]
4-Vinylsyringol	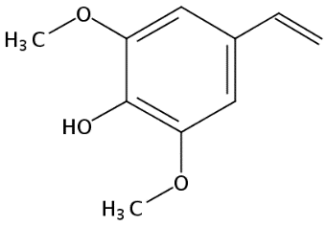	-	[43]
Syringaldehyde	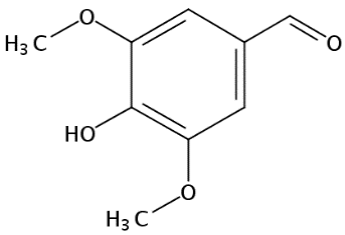	95.8	[43]
4-Ethylsyringol	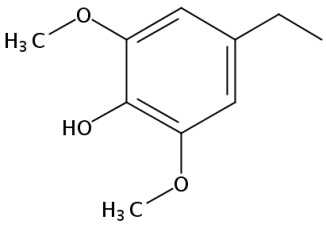	-	[43]

Dihydroconiferyl alcohol	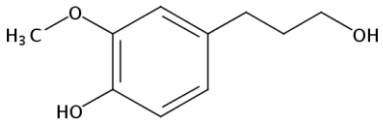	-	[43]
Methoxy eugenol	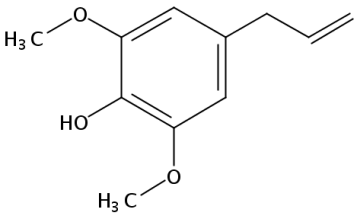	90.5	[43]
***trans*-4-Propenylsyringol**	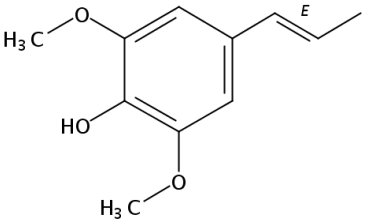	-	[43]
***cis*-4-Propenylsyringol**	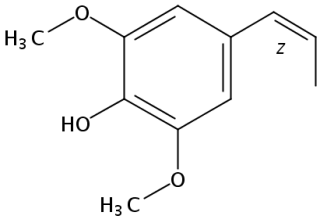	-	[43]
Acetosyringone	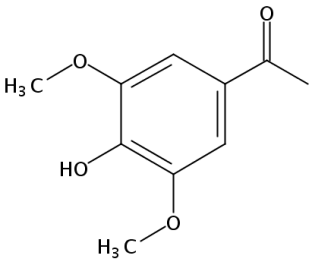	93.5	[43]
4-Propylsyringol	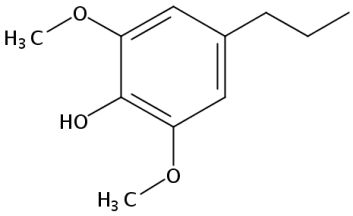	-	[43]
Syringylacetone	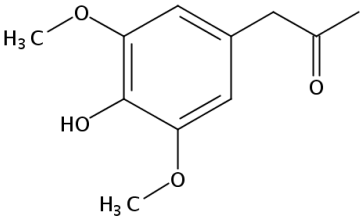	-	[43]

Propiosyringone	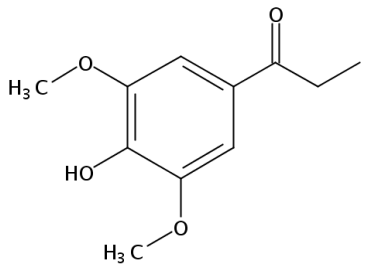	-	[43]
***trans*-Sinapyl alcohol**	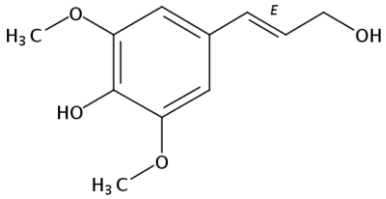	-	[43]
Dihydrosinapyl alcohol	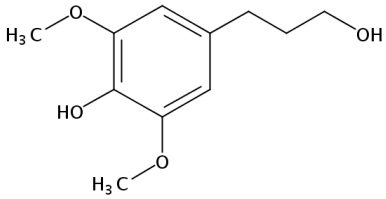	-	[43]

In Table 7, the list of 24 identified and suggested compounds is presented, based in GC-MS analysis of evaporated light bio-oil reaction product sorted in ascending molecular weight. Only 7 compounds were positively identified using standard solutions: guaiacol, 4-methylguaiacol, vanillin, 4-ethylguaiacol, syringol, *trans*-isoeugenol, and 4-propylguaiacol. Outside of those, 3 represented a match factor in the NIST database above 90% in spectra. The remaining 14 compounds were suggested based on spectra comparison with literature [43].

All of the identified compounds were monomers. There were more compounds registered in the MS spectra of the light bio-oil samples – presumably dimers – however, they failed to be identified. The chromatograms can be found in Appendix 5–7.

Table 8. Identified and suggested compounds sorted by ascending molecular weight and their relative abundance (area % of identified compounds) for each experiment.

		Relative abundance (area %)		
M (g/mol)	**Compound**	**Pd/C 3%**	**ZrO_2**	**Pd/Al_2O_3 5%**
124.14	**Guaiacol**	-	1.69	0.95
138.16	**4-Methylguaiacol**	1.26	3.04	2.12
152.15	**Vanillin**	-	1.61	-
152.19	**4-Ethylguaiacol**	1.38	1.62	2.34
154.16	**Syringol**	3.75	6.67	4.47
164.20	**Eugenol**	-	1.02	-
164.20	**trans-Isoeugenol**	-	7.41	-
166.17	**Acetovanillone**	-	1.07	-
166.22	**4-Propylguaiacol**	7.97	1.06	4.87
168.19	**4-methylsyringol**	6.73	9.47	7.08
180.20	**Guaiacylacetone**	-	1.28	-
180.20	**4-Vinylsyringol**	-	1.78	-
182.17	**Syringaldehyde**	-	7.29	0.88
182.22	**4-Ethylsyringol**	5.68	4.02	6.44
182.22	**Dihydroconiferyl alcohol**	6.31	1.19	8.5
194.23	**Methoxyeugenol**	-	3.59	-
194.23	**trans-4-Propenylsyringol**	-	22.05	-
194.23	**cis-4-propenyl-syringol**	2.27	-	1.19
196.20	**Acetosyringone**	1.48	4.34	1.68
196.24	**4-Propylsyringol**	35.39	3.96	18.94
210.23	**Syringyl acetone**	1.21	3.9	1.16
210.23	**Propiosyringone**	1.71	1.81	1.96
210.23	**trans-Sinapyl alcohol**	-	4.15	1.05
212.24	**Dihydrosinapyl alcohol**	24.85	5.96	36.38

Table 8 contains the relative abundance of the GC-MS indentified and suggested compounds in all experiments. The experiment involving the ZrO_2 catalyst yielded the highest variety of identified compounds, especially resulting in more guaiacol derivatives than the others. The relative abundances in each experiment were calculated with respect to the total area of identified compounds in that experiment, therefore, the abundances may not be compared directly, but as which compounds are more prominent per sample.

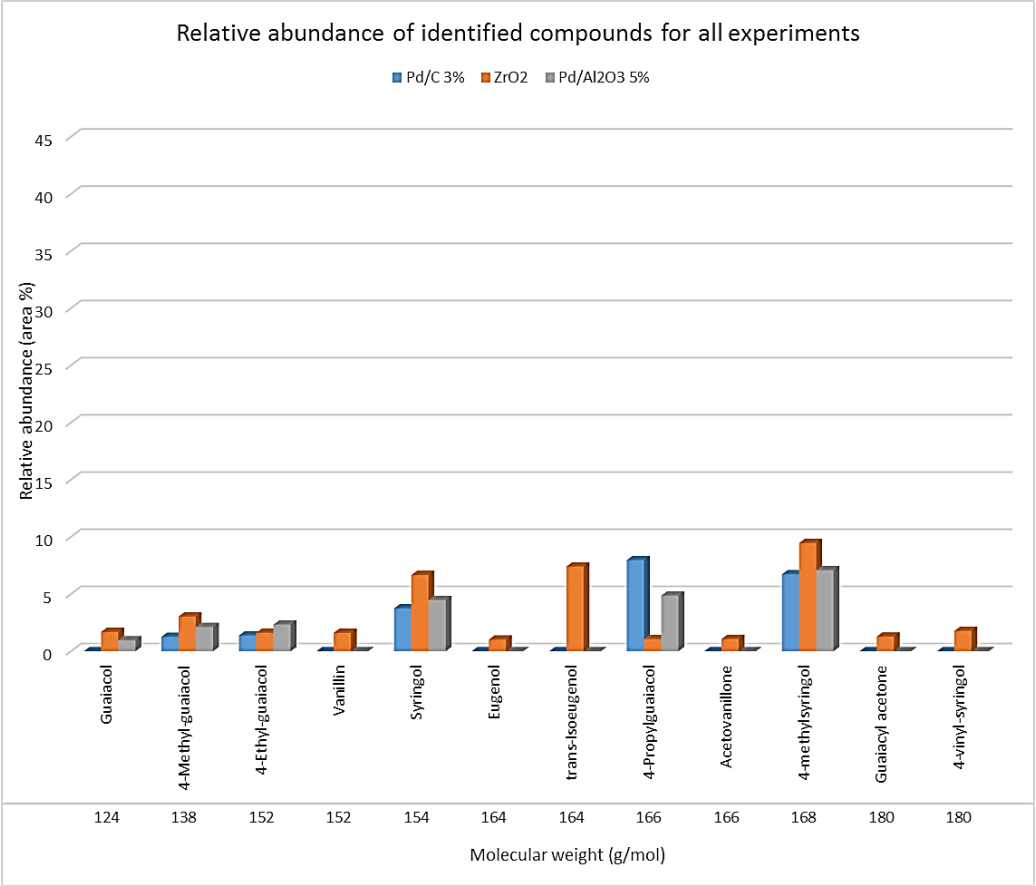

Figure 25. Relative abundance of identified compounds on evaporated light bio-oil for each experiment for the range [124–180] g/mol of molecular weight.

In Figures 25 and 26 the relative abundances (area %) of the GC-MS identified compounds in the evaporated light bio-oil reaction product are displayed. Figure 25 is comprised of the compounds with molecular weight range of 124–180 g/mol, and Figure 26 of those of molecular weight in the range of 182–238 g/mol. The undivided graph can be found in Appendix 3.

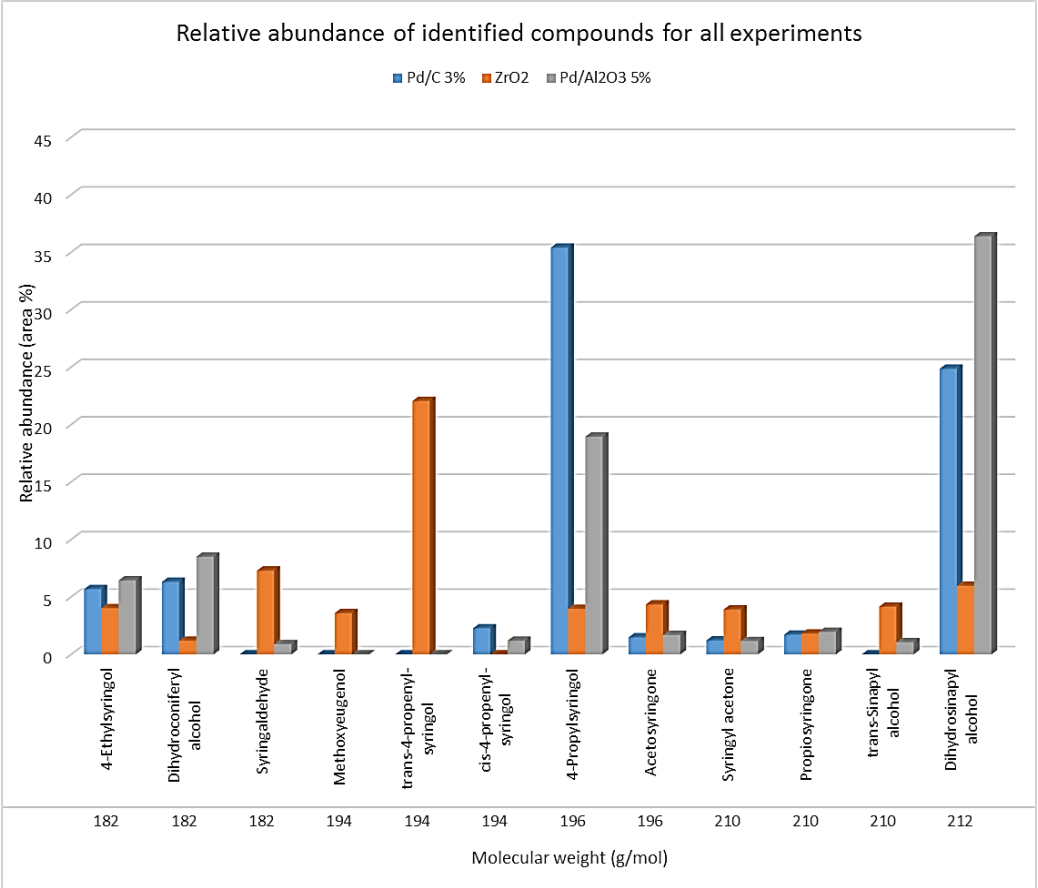

Figure 26. Relative abundance of identified compounds on evaporated light bio-oil for each experiment for the range [182–238] g/mol of molecular weight.

As mentioned previously, the bio-oil that resulted from the experiment involving the ZrO_2 catalyst contains more identified compounds than the others, with highest amount of *trans*-4-propenylsyringol. Regarding the experiments involving the Pd/C 3% and Pd/ Al_2O_3 5% catalyst, the highest abundances for both are 4-propylsyringol, more representative to the Pd/C 3% experiment, as well as dihydrosinapyl alcohol, more representative to the Pd/ Al_2O_3 5% experiment.

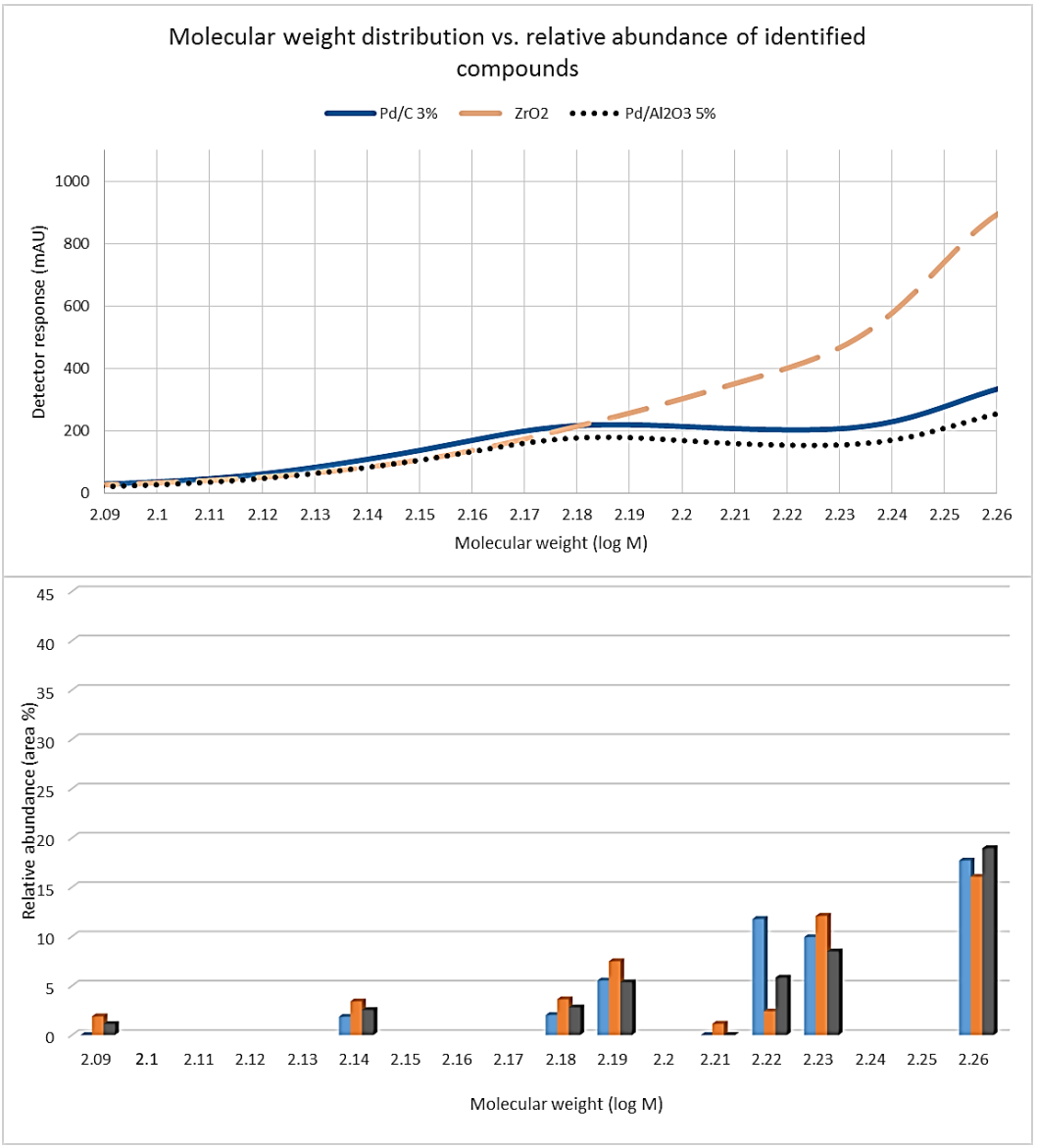

Figure 27. Comparison of the relative abundance of identified compounds and the molecular weight distribution of evaporated light bio-oil for each experiment for the range [124–180] g/mol of molecular weight.

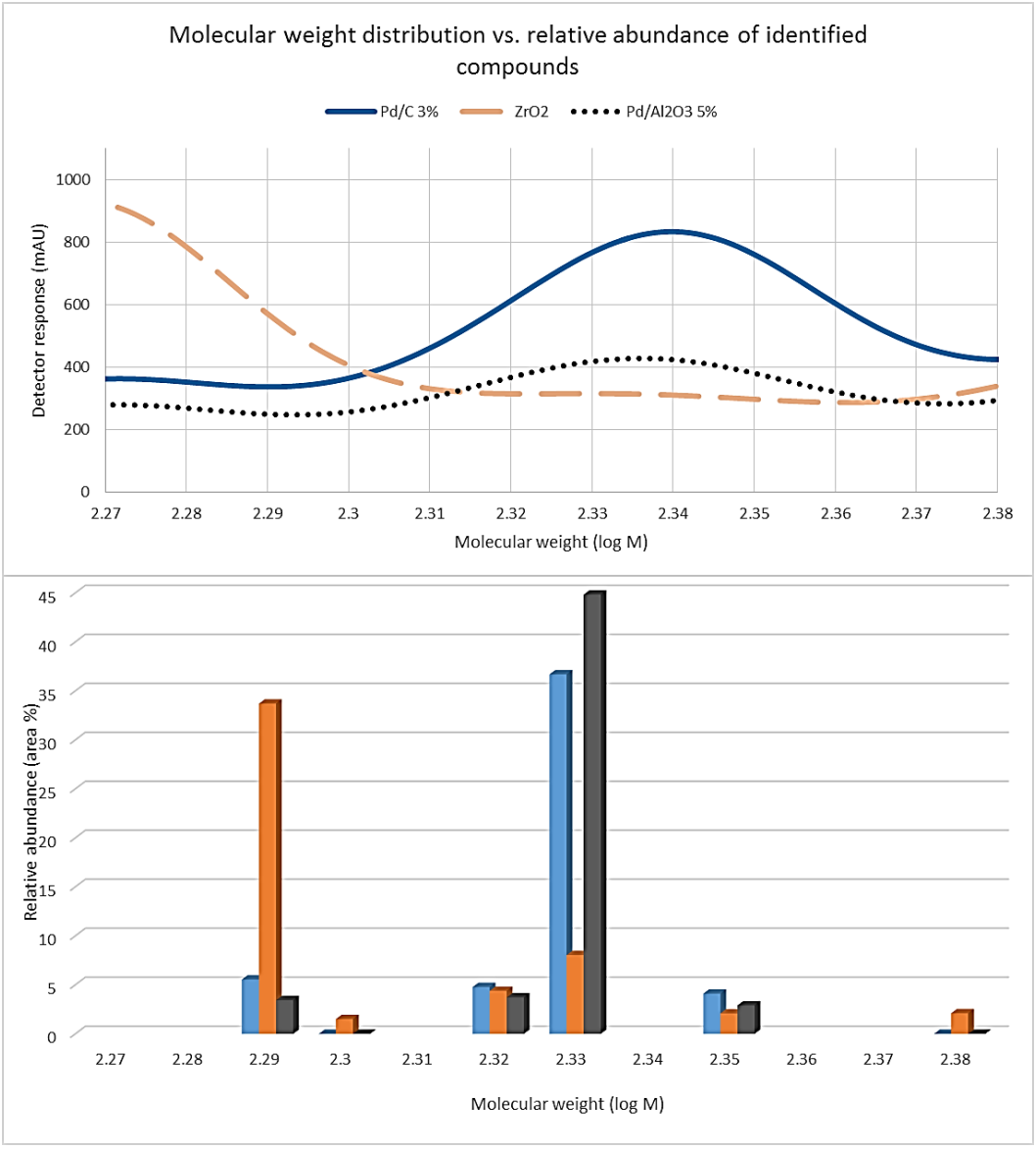

Figure 28. Comparison of the relative abundance of identified compounds and the molecular weight distri-bution of evaporated light bio-oil for each experiment for the range [182–238] g/mol of molecular weight.

In Figures 27 and 28, a comparison between the compounds separated by gas chromatography and identified by a mass spectroscopy detector – translated in their logarithmic molecular weights – against the molecular weight distribution identified by a variable wavelength detector of the compounds separated by gel permeation chromatography is shown. Figure 27 encompasses the range of molecular weights [124–180] g/mol – or logarithmic range [2.09–2.26] – and Figure 28 that of [182–238] g/mol, or logarithmic range [2.26–2.38]. The undivided graph can be found in Appendix 4.

The respective profiles of component abundance seem to reasonably match for all experiments individually, utmost for the Pd/Al_2O_3 experiment. The most outstanding incongruities belong to the ZrO_2 experiment, being that according to the GPC-VWD results, the peaks at 2.23 and 2.26 log M should be considerably higher in the GC-MS results. For the Pd/C 3% experiment, the highest difference in profiles can be observed at 2.29 log M, which peak for the GC-MS should be smaller when compared to the GPC-VWD distribution.

When comparing the distributions for all experiments, the relative abundances display a greater amount of mismatches. However, as mentioned above, the relative abundances of the GC-MS in each experiment were calculated with respect to the total area of identified compounds in that experiment, therefore, the abundances may not be compared directly, but as which compounds are more prominent per sample.

6. Conclusions

In the broadest vision to contribute to sustainability, with focus on the use of lignin as a sustainable source for the production of chemicals, a literature review was carried out in the scope of lignin, its extraction, and decomposition. Experiments were performed to find which chemicals may potentially be produced from isolated (organosolv-extracted) lignin through its decomposition by hydrodeoxygenation, as well as to describe the properties and composition of the product as a whole, including its unidentified components. Catalyst screening was implemented to evaluate the optimal catalyst to obtain low molecular weight organic compounds.

6.1 General discussion of results

Four product streams were analyzed resulting from the hydrodeoxygenation reaction of lignin and ethanol: gas product, light bio-oil, heavy bio-oil, and char. Regarding the properties and composition of the liquid reaction product, four parameters were considered: number-average molecular weight, weight-average molecular weight, polydispersity index (PDI), and a custom-defined fraction of light (monomers and dimers) and heavy (trimers and bigger oligomers) compounds. These properties were first compared for the “light bio-oil” (ethanol soluble) and “heavy bio-oil” (ethanol insoluble but THF soluble) product fractions for each experiment individually. The results show that the light bio-oil (ethanol soluble) product fraction is more relevant for the purpose of isolating small molecular weight compounds based on their average molecular weight. Futhermore, the heavy bio-oil product fraction represents less than 5% the amount of light bio-oil in all experiments.

Analysis of the polydispersity index (PDI) showed a wider molecular weight distribution for the heavy bio-oil product fraction in all experiments. For the perspective of separation, higher molecular weight differences suggests high differences in boiling points, opening the possibility to separation by distillation, so the heavy bio-oil fraction would be easier to separate. However, from the perspective of future chemical treatment for direct applications, the lower PDI of the light bio-oil

represents a good result. Another source to conclude that the heavy bio-oil fraction would be easier to separate comes from the graphical comparison distributions, where a clear bimodal molecular weight distribution of the heavy bio-oil fraction may represent ease of separation of at least these two segments, for example by solvent-non-solvent fractionation or by vacuum distillation [42].

Aside from the catalyst screening, the effect of evaporation of samples to obtain solvent-free light bio-oil was investigated. The results showed a shift in molecular weight distribution and averages towards higher molecular weights for the evaporated samples, which may be attributed to evaporation of small molecular weight volatiles, including potentially valuable aromatics. In regards to the criteria of minimum loss of product in evaporation, Pd/Al_2O_3 5% displayed the best performance.

Regarding polydispersity, the evaporated samples showed and increase compared to those fresh from the reaction. If light compounds are evaporated and lost, the range of molecular weight should decrease. However, an increase in polydispersity suggests a rearrangement of molecules, in other words, the product either reacts with oxygen as it evaporates over time and/or it recombines and oligomerizes at room temperature.

The catalyst screening results were focused on the evaporated light bio-oil product fraction, and showed lowest molecular weight for the experiment involving the Pd/C 3% catalyst with values of 363.4 g/mol of number average and 583.9 g/mol of weight average, as well as fraction of light (monomers and dimers) compounds of 24.1%. The experiment involving the Pd/Al_2O_3 5% showed the highest molecular weights and lowest light compounds fraction. The difference in polydispersity for all experiments was not significant.

Regarding the gas product, the experiment involving the Pd/Al_2O_3 5% catalyst exhibited a considerably high amount of methane, and a considerably low amount of hydrogen concentration compared to the other experiments. The decrease in hydrogen and increase in methane could be attributed to a higher hydrogenation activity of the Pd/Al_2O_3 5% catalyst, resulting in severe fractionation of the aromatic side chains, including methyl/methoxy substitutions.

In regards to the mass balance of the product streams excluding the gas phase, the Pd/Al_2O_3 5% catalyst showed the highest amount of light bio-oil, however, also the highest amount of char. On the other hand, the lowest amounts of both light bio-oil and char belonged to the experiment involving the Pd/C 3% catalyst.

Considering that the same experiment exhibited highest amount of methane and lowest amount of hydrogen concentration in the gas product, as well as highest molecular weights, lowest fraction of light compounds, and lowest change in molecular weight from evaporation in the light bio-oil product fraction, all the results except the mass balance point to the conclusion of the high hydrogenation activity of the Pd/Al_2O_3 5% that caused heavy losses in small molecular weight compounds. Perhaps the mass balance results are corrupted with human error both in evaporation and filtration. Another possibility is that disregarding the results of the gas product composition, a possible conclusion is that the catalyst aids in the recombination/oligomerization process, and the high molecular weights are not due to small molecular weight compounds lost as small volatile hydrocarbons, but as repolymerized molecules.

The last section of experimental results dealt with identification of compounds by GC-MS. Seven compounds were positively identified using standard solutions: guaiacol, 4-methylguaiacol, vanillin, 4-ethylguaiacol, syringol, trans-isoeugenol, and 4-propylguaiacol. Outside of those, 3 represented a match factor in the NIST database above 90% in spectra. The remaining 14 compounds were suggested based on spectra comparison with literature [43]. The most representative compounds for the experiments involving the Pd/C 3%, ZrO2, and Pd/Al_2O_3 5% catalysts are 4-propylsyiringol, trans-4-propenylsyringol, and dihydrosinapyl alcohol, respectively.

6.2 Error sources in the experimental work

The most important error source regarding the experimental work is the loss by volatilization of small molecular weight compounds. Results show not only an increase in molecular weight by evaporation, but also recondensation. Depending on how carefully the product recovery, vacuum filtrations, and container transfers are done, the mass balance results may prove very variable.

In the graphical comparison of the molecular weight distributions was observed an overlap between the profiles of both light and heavy product fractions in all experiments, meaning that there's a considerable amount of relatively lower molecular weight molecules in the heavy fraction. A part of this could be attributed to deficiency in the filtration, as some ethanol solubles carried out with the insolubles that were afterward extracted with THF.

Another source of error was the evaporation rate of the samples. At least two samples each of 0.5 g, 1 g, and 2 g were left in a fume hood, and the average of concentration was used to calculate the light bio-oil (ethanol soluble reaction product) for the mass balance. However, the samples showed different evaporation rates, and three days may not have been enough to accurately estimate the amount of light bio-oil fraction.

Regarding the gas sampling, shortcomings in valves installations led to air entering the sample with reactor product in the first sampling directly from the reactor system, as well as during analysis in the GC-TCD.

6.3 Suggestion for further studies

Regarding the same analyses performed in this work, the first path to further studies is to screen more catalysts and evaluate their performance in production of small molecular weight aromatics. A set of noble metals in the same support, as well as a set of supports with the same metal are possibilities.

Regarding more analyses, the light bio-oil may be subjected to Karl Fischer analysis to determine the water content of the fresh ethanol soluble phase of reaction product. Analysis of the char should prove useful in discovering the reaction pathways of lignin depolymerization through hydrodeoxygenation. Finally, the gas product could be subjected to continuous Fourier Transform Infrared (FT-IR) analysis to measure the development of gas concentrations during the reaction.

References

[1] International Energy Agency. *Key World Energy Statistics*. Chirat: France, 2014.

[2] Menon, V. and Rao, M., Trends in bioconversion of lignocellulose: Biofuels, platform chemicals & biorefinery concept, *Prog. Energy Combust. Sci.* **38** (2012) 522–550.

[3] Peltola, A. (Ed.). *Metsätilastollinen vuosikirja 2014*. Metsäntutkimuslaitos: Finland, 2014.

[4] Oinonen, P., Zhang, L., Lawoko, M., and Henriksson, G., On the formation of lignin polysaccharide networks in Norway spruce. *Phytochemistry* **111** (2015) 177–184.

[5] Carmona, C., Langan, P., Smith, J. C., and Petridis, L., Why genetic modification of lignin leads to low-recalcitrance biomass. *Phys. Chem. Chem. Phys.* **17** (2015) 358–364.

[6] Bland, D. E. and Logan, A. F., The properties of Syringyl, Guaiacyl and p-Hydroxyphenyl Artificial Lignins. *Biochem. J.* **95** (1965) 515–520.

[7] Zhu, W. and Theliander, H., Precipitation of Lignin from Softwood Black Liquor: An Investigation of the Equilibrium and Molecular Properties of Lignin. *BioResources* **10** (2015) 1696–1714.

[8] Taherzadeh, M. J. and Karimi, K., Pretreatment of Lignocellulosic Wastes to Improve Ethanol and Biogas Production: A Review. *Int. J. Mol. Sci.* **9** (2008) 1621–1651.

[9] Cybulska, I., Brudecki, G., Rosentrater, K., Julson, J. L., and Lei, H., Comparative study of organosolv lignin extracted from prairie cordgrass, switchgrass and corn stover. *Bioresour. Technol.* **118** (2012) 30–36.

[10] Ek, M., Gellerstedt, G., and Henriksson, G. (Eds.), *Wood chemistry and biotechnology*, Pulp and Paper Chemistry and Technology vol. 1, De Gruyter: Berlin, 2009, 308 p.

[11] Pandey, M. P. and Kim, C. S., Lignin Depolymerization and Conversion: A Review of Thermochemical Methods. *Chem. Eng. Technol.* **34** (2011) 29–41.

[12] Zakzeski, J., Bruijnincx, P. C. A., Jongerius, A. L., and Weckhuysen, B. M., The Catalytic Valorization of Lignin for the Production of Renewable Chemicals. *Chem. Rev.* **110** (2010) 3552–3599.

[13] Laskar, D. D. and Yang, B., Pathways for biomass-derived lignin to hydrocarbon fuels. *Biofuels, Bioprod. Biorefin.* **7** (2013) 602–626.

[14] Du, X., Pérez-Boada, M., Fernández, C., Rencoret, J., del Río, J. C., Jiménez-Barbero, J., Li, J., Gutiérrez, A., and Martínez, A. T., Analysis of lignin-carbohydrate and lignin-lignin linkages after hydrolase treatment of xylan-lignin, glucomannan-lignin and glucan-lignin complexes form spruce wood. *Planta* **239** (2014) 1079–1090.

[15] Biermann, C. J., *Handbook of pulping and papermaking*. 2nd Ed., Academic Press, Elsevier: California, U.S.A., 1996.

[16] Metso. *Metso-supplied world's first commercial LignoBoost plant succesfully starts up at Domtar in the USA*. April 30, 2013. http://www.metso.com/News/Newsdocuments.nsf/web3newsdoc/DC7908091C20A480C2257B5D002B52BD. Accessed on March 3, 2015.

[17] Bundhoo, Z. M. A., Mudhoo, A., and Mohee, R., Promising Unconventional Pretreatments for Lignocellulosic Biomass. *Crit. Rev. Environ. Sci. Technol.* **43** (2013) 2140–2211.

[18] Ximenes, F. A., Gardner, W. D., and Cowie, A. L., The decomposition of wood products in landfills in Sydney, Australia. *Waste Manage.* **28** (2008) 2344–2354.

[19] Schwanninger, M. and Hinterstoisser, B., Klason Lignin: Modifications to Improve the Precision of the Standardized Determination. *Holzforschung* **56** (2002) 161–166.

[20] Sluiter, J. B., Ruiz, R. O., Scarlata, C. J., Sluiter, A. D., Templeton, D. W., Compositional Analysis of Lignocellulosic Feedstocks. 1. Review and Description of Methods. *J. Agric. Food Chem.* **58** (2010) 9043–9053.

[21] Espinoza-Acosta, J. L., Torres-Chávez, P. I., Carvajal-Millán, E., Ramírez-Wong, B., Bello-Pérez, L. A., and Montaño-Leyva, B., Ionic Liquids and Organic Solvents for Recovering Lignin from Lignocellulosic Biomass. *BioResources* **9** (2014) 3660–3687.

[22] Mora-Pale, M., Meli, L., Doherty, T. V., Linhardt, R. J., and Dordick, J. S., Room Temperature Ionic Liquids as Emerging Solvents for the Pretreat-

ment of Lignocellulosic Biomass. *Biotechnol. Bioeng.* **108** (2011) 1229–1245.

[23] Long, J., Li, X., Guo, B., Wang, L., and Zhang, N., Catalytic delignification of sugarcane bagassein the presenceof acidic ionic liquids. *Catal. Today* **200** (2013) 99–105.

[24] Krogell, J., Holmbom, B., Pranovich, A., Hemming, J., and Willför, S., Extraction and chemical characterization of Norway spruce inner and outer bark. *Nord. Pulp Pap. Res. J.* **27** (2012) 6–17.

[25] Ma, R., Xu, Y., and Zhang, X., Catalytic Oxidation of Biorefinery Lignin to Value-added Chemicals to Support Sustainable Biofuel Production. *ChemSusChem* **8** (2015), 24–51.

[26] Chávez-Sifontes, M. and Domine, M. E., Lignin, structure and applications: depolymerization methods for obtaining aromatic derivatives of industrial interest. *Avances en Ciencias e Ingeniería* **4** (2013) 15–46.

[27] Gasser, C. A., Hommes, G., Schäffer, A., and Corvini, P., F.-X., Multicatalysis reactions: new propsects and challenges of biotechnology to valorize lignin. *Appl. Microbiol. Biotechnol.* **95** (2012) 1115–1134.

[28] Hofrichter, M., Review: lignin conversion by manganese peroxidase (MnP). *Enzyme Microb. Technol.* **30** (2002) 454–466.

[29] Roberts, V., Fendt, S., Lemonidou, A. A., Li, X., and Lercher, J. A., Influence of alkali carbonates on benzyl phenyl ether cleavage pathways in superheated water. *Applied Catalysis B: Environmental* **95** (2010) 71–77.

[30] Yang, L., Li, Y., and Savage, P. E., Hydrolytic Cleavage of C-O Linkages in Lignin Model Compounds Catalyzed by Water-Tolerant Lewis Acids. *Ind. Eng. Chem. Res.* **53** (2014) 2633–2639.

[31] Roberts, V. M., Stein, V., Reiner, T., Lemonidou, A., Li, X., and Lercher, J. A., Towards Quantitative Catalytic Lignin Depolymerization. *Chem. Eur. J.* **17** (2011) 5939–5948.

[32] Toledano, A., Serrano, L., and Labidi, J., Organosolv lignin depolymerizataion with different base catalysts. *J. Chem. Technol. Biotechnol.* **87** (2012) 1593–1599.

[33] Zhu, Z., and Zhu, J., Catalytic oxygen atom transfer from lignin to cellulose and hemicellulose and its importance in biorefining. *Fuel* **148** (2015) 226–230.

[34] Elliott, D. C., Historical Developments in Hydroprocessing Bio-oils. *Energy Fuels* **21** (2007) 1792–1815.

[35] Werhan, H., Mir, J. M., Voitl, T., and von Rohr, P. R., Acidic oxidation of kraft lignin into aromatic monomers catalyzed by transition metal salts. *Holzforschung* **65** (2011) 703–709.

[36] Brebu, M. and Vasile, C., Thermal degradation of lignin – a review. *Cellul. Chem. Technol.* **44** (2010) 353–363.

[37] Cho, J., Chu, S., Dauenhauer, P. J., and Huber, G. W., Kinetics and reaction chemistry for slow pyrolysis of enxymatic hydrolysis lignin and organosolv extracted lignin derived from maplewood. *Green Chem.* **14** (2012) 428–439.

[38] Choi, H. S., Meier, D., and Windt, M., Rapid Screening of Catalytic Pyrolysis Reactions of Organosolv Lignins with the vTI-Mini Fast Pyrolyzer. *Environ. Prog. Sustainable Energy* **31** (2012) 240–244.

[39] Sarwar Jahan, M. and Phil Mun, S., Isolation and Characterization of Lignin from Tropical and Temperate Hardwood. *Bangladesh J. Sci. Ind. Res.* **44** (2009) 271–280.

[40] Lange, H., Rulli, F., and Crestini, C., *Why "laboratory standard" is not good enough in GPC-analyses of lignins* [Abstract]. 249th ACS National Meeting & Exposition: United States, 2015.

[41] Ang, A., Ashaari, Z., Bakar, E. S., and Ibrahim, N. A., Characterization and Optimization of the Glyoxalation of a Methanol-Fractionated Alkali Lignin using Response Surface Methodology. *BioResources* **10** (2015) 4795–4810.

[42] Scicchitano, M. and Turri, S., Cyclic acetals of fluorinated polyether macrodiols. *J. Fluorine Chem.* **95** (1999) 97–103.

[43] Faix, O., Meier, D., and Fortmann, I., Gas chromatographic separation and mass spectrometric characterization of monomeric lignin derived products. *Holz Roh- Werkst.* **48** (1990) 281–285.

Appendix 1 – GPC standard solution “STD A” chromatogram

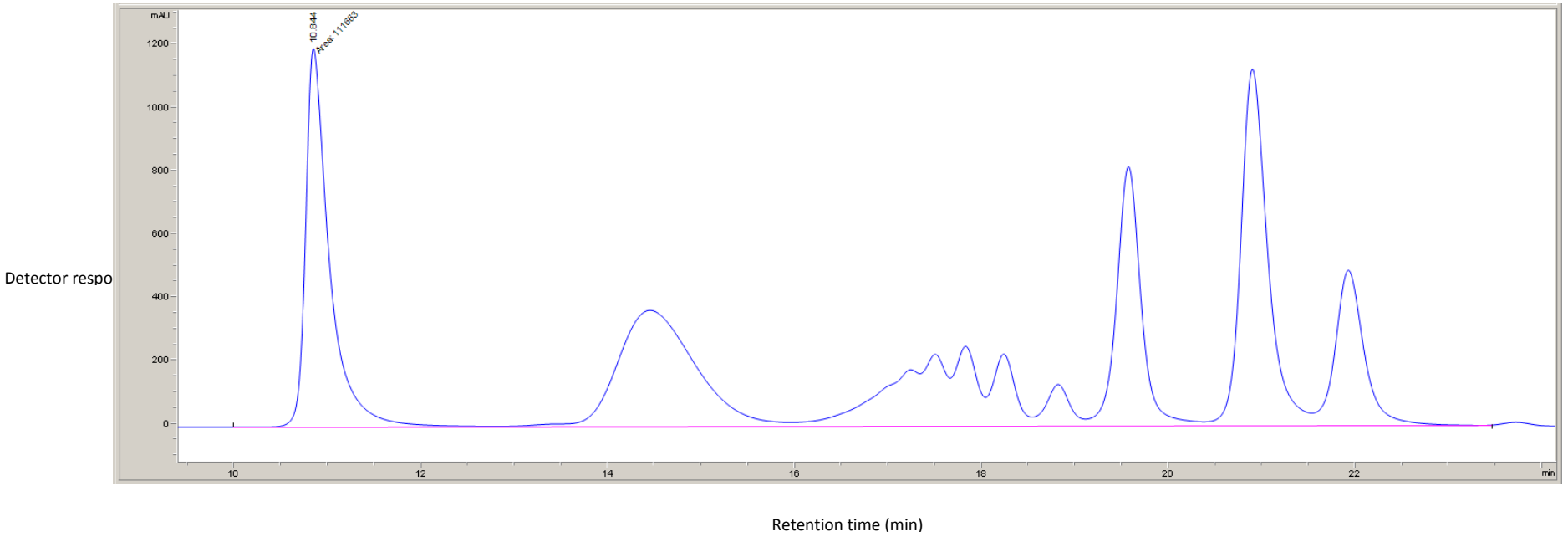

Figure 29. GPC chromatogram of the standard solution “STDA” used for calibration.

Appendix 2 – GPC standard solution “STD B” chromatogram

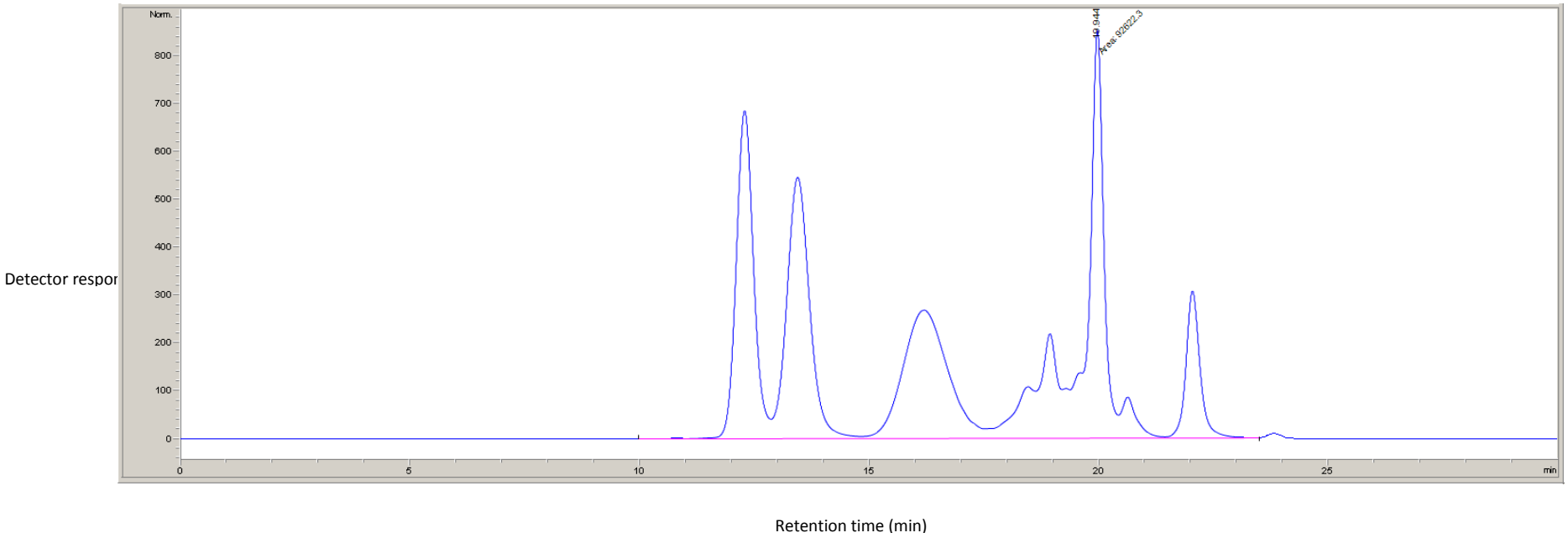

Figure 30. GPC chromatogram of the standard solution “STDB” used for calibration.

Appendix 3 – GC-MS identified compounds

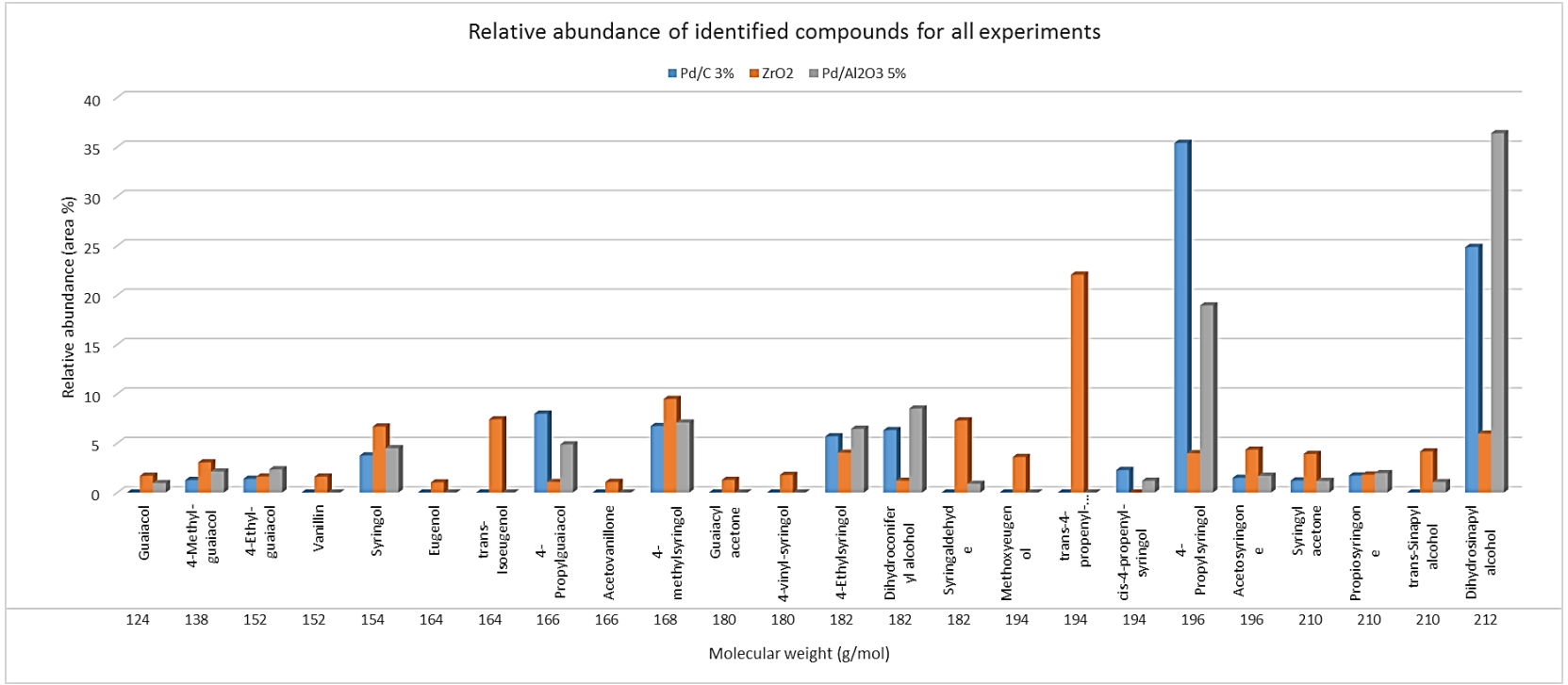

Figure 31. Relative abundance of identified compounds on evaporated light bio-oil for each experiment and their molecular weights.

Appendix 4 – GC-MS identified compounds vs. GPC MW distribution

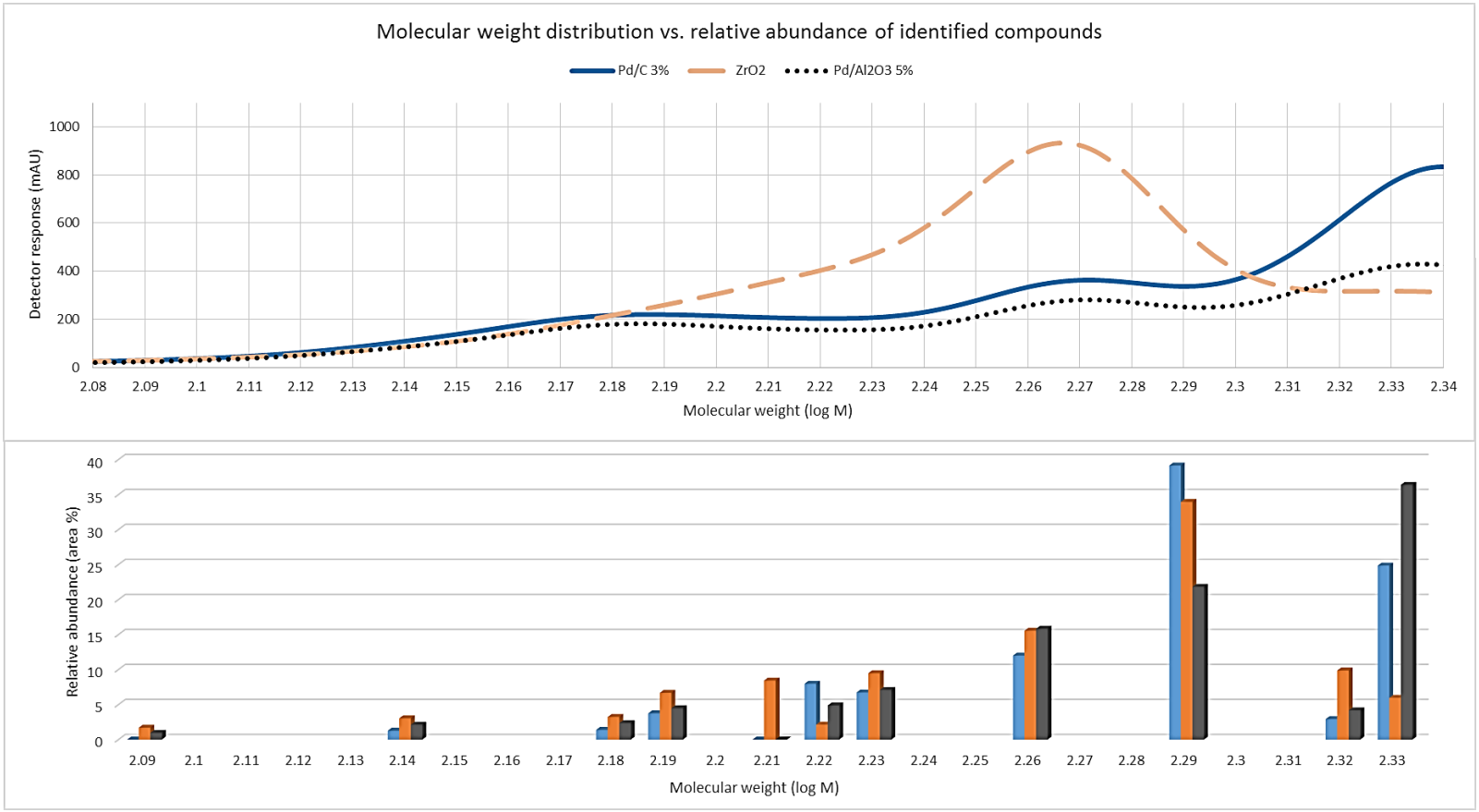

Figure 32. Comparison of the relative abundance of identified compounds and the molecular weight distri-bution of evaporated light bio-oil for each experiment.

Appendix 5 – GC-MS chromatogram for the experiment involving the Pd/C 3% catalyst

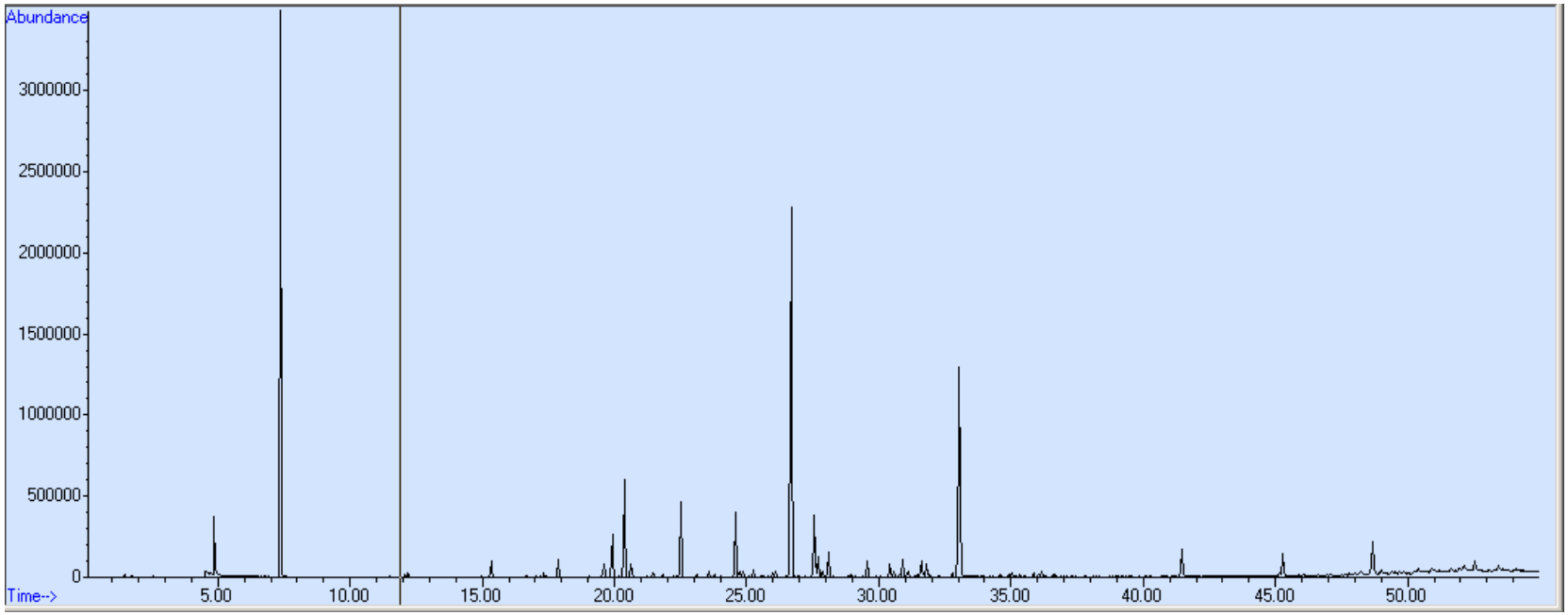

Retention time (min)

Appendix 6 – GC-MS chromatogram for the experiment involving the ZrO_2 catalyst

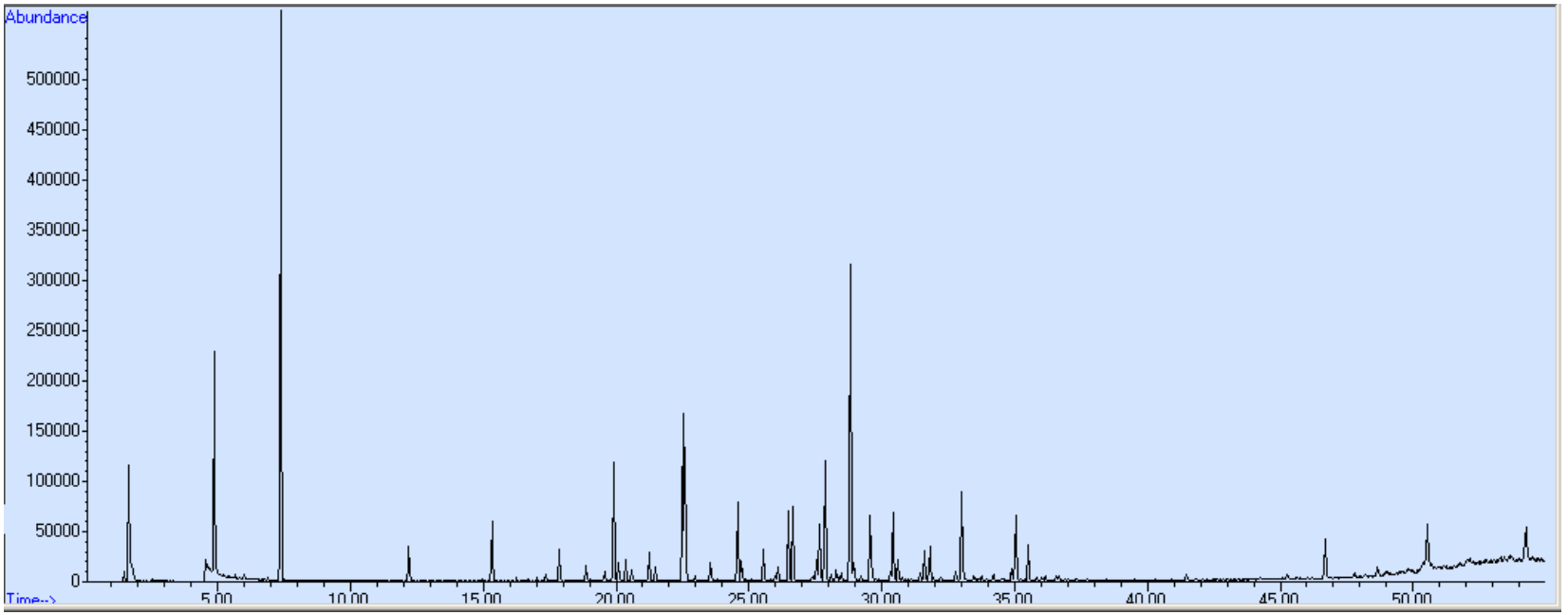

Retention time (min)

Appendix 7 – GC-MS chromatogram for the experiment involving the Pd/Al_2O_3 catalyst

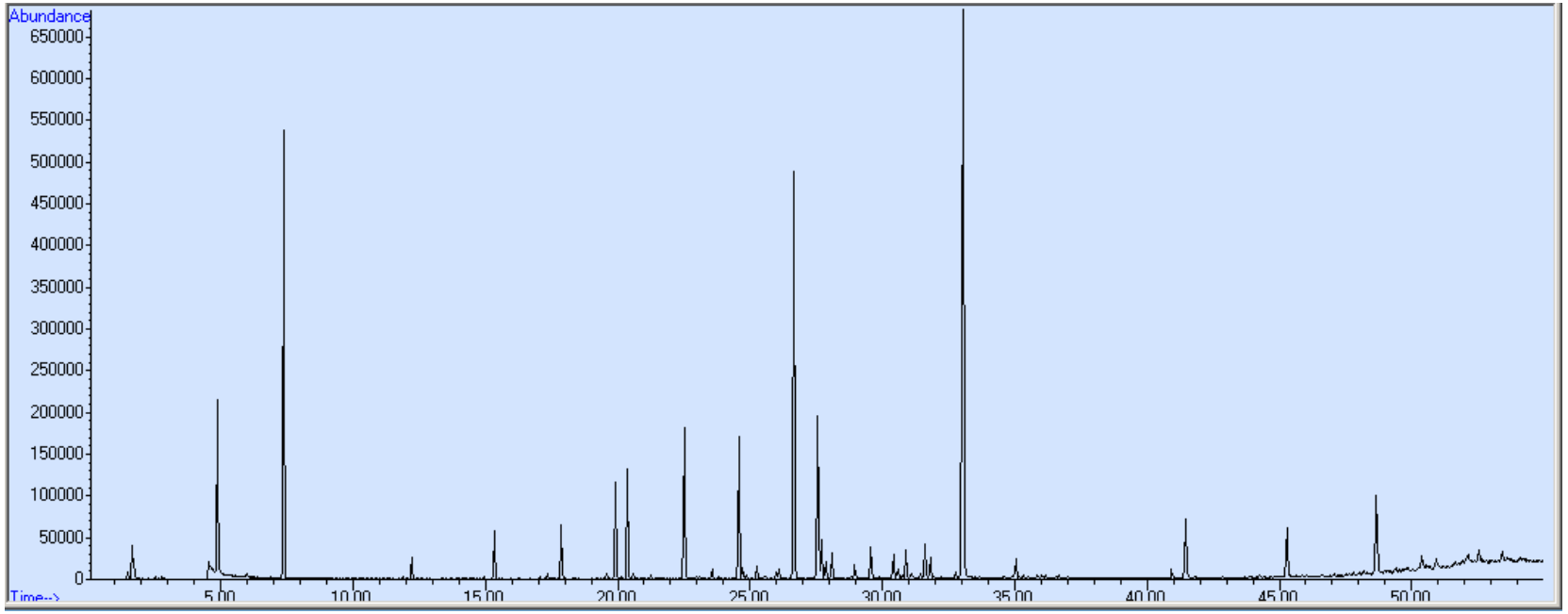

Retention time (min)

Appendix 8 – Business potential

Aside from the contribution to sustainability of using abundant lignocellulosic biomass feedstock to produce energy and chemicals instead of fossil resources facing depletion, the work of this thesis may also have business potential.

Lignin is a side-product of paper making, currently used in biorefinery schemes as fuel, to provide energy for internal use. The experimental work carried here involved upgrading lignin into potentially valuable small molecular weight chemicals. Although in the present this methodology may not be suitable at industrial levels due to relatively high hydrogen prices, finding the optimal catalyst to depolymerize lignin may be of utmost importance if and when fossil fuel prices rise to unsustainable levels and lignin is required to fulfill the role as source for bio-based materials and products, completely replacing fossil fuels.